OPEN ACCESS
IOP Publishing
Journal of Physics A: Mathematical and Theoretical
J. Phys. A: Math. Theor. **54** (2021) 375201 (29pp)
https://doi.org/10.1088/1751-8121/ac0983

The square lattice Ising model on the rectangle III: Hankel and Toeplitz determinants

Alfred Hucht*

Faculty of Physics, University of Duisburg-Essen, 47048 Duisburg, Germany

E-mail: fred@thp.uni-due.de

Received 29 March 2021, revised 27 May 2021
Accepted for publication 9 June 2021
Published 3 September 2021

Abstract

Based on the results obtained in (Hucht 2017 *J. Phys.* A*: Math. Theor.* **50** 065201), we show that the partition function of the anisotropic square lattice Ising model on the $L \times M$ rectangle, with open boundary conditions in both directions, is given by the determinant of an $M/2 \times M/2$ Hankel matrix, that equivalently can be written as the Pfaffian of a skew-symmetric $M \times M$ Toeplitz matrix. The $M - 1$ independent matrix elements of both matrices are Fourier coefficients of a certain symbol function, which is given by the ratio of two characteristic polynomials. These polynomials are associated to the different directions of the system, encode the respective boundary conditions, and are directly related through the symmetry of the considered Ising model under exchange of the two directions. The results can be generalized to other boundary conditions and are well suited for the analysis of finite-size scaling functions in the critical scaling limit using Szegő's theorem.

Keywords: Hankel matrix, Toeplitz matrix, exact solution, open boundary conditions, square lattice Ising model, transfer matrix, determinant

(Some figures may appear in colour only in the online journal)

1. Introduction

The anisotropic two-dimensional Ising model [1] on the $L \times M$ square lattice is one of the best investigated models in statistical mechanics. In the thermodynamic limit $L, M \to \infty$, it has a continuous phase transition, from a disordered high-temperature phase to an ordered

*Author to whom any correspondence should be addressed.

low-temperature phase, at a critical temperature T_c. After the exact solution of the periodic case by Onsager and Kaufman [2, 3], many authors have contributed to the knowledge about this model under various aspects, such as different boundary conditions (BCs) or surface effects [4–6].

Until some years ago, exact solutions for arbitrary temperatures were only known for systems with periodic or antiperiodic BCs in at least one direction, as then a Fourier transform along this translationally invariant direction could be used to diagonalize the problem in the corresponding direction. The remaining direction could be handled afterwards with a transfer matrix method, involving a 2×2 transfer matrix, taking into account arbitrary BCs, or even line disorder [4].

This changed in 2016, when Baxter [7, 8] and Hucht [9–11] independently presented exact results for the Ising model on the rectangle, with open BCs in both directions, expressing the partition function as $M \times M$ and $M/2 \times M/2$ determinants, respectively. While Baxter used Kaufman's spinor method [3] below T_c and focused on the thermodynamic limit [7], where he exactly calculated the corner contributions to the free energy conjectured in [12], Hucht utilized the dimer method of McCoy *et al* [4, 13–16], combined with Schur reductions and a block transfer matrix formulation of Molinari [17], and derived closed expressions for finite systems at arbitrary temperatures. The resulting transfer matrices directly correspond to the spinor method matrices, bridging the gap between these so far rather unrelated methods.

Near the critical temperature T_c, the direction-dependent bulk correlation length of thermal fluctuations $\xi^\delta_\infty(T)$ diverges according to $\xi^\delta_\infty(T > T_c) \simeq \xi^\delta_0(T/T_c - 1)^{-\nu}$, where $\delta = \leftrightarrow, \updownarrow$ denotes the directions corresponding to L and M, ξ^δ_0 are interaction-dependent metric factors, and the correlation length critical exponent is $\nu = 1$ in the two-dimensional Ising model[1]. If $\xi^{\leftrightarrow,\updownarrow}_\infty(T)$ is of the order of (or larger as) the respective system size L or M, interesting finite-size effects such as the critical Casimir effect emerge, which describes interactions of the system boundaries mediated by long-range critical fluctuations [18, 19] in close analogy to the quantum electrodynamical Casimir effect [20, 21]. These finite-size effects can be described [22] by universal finite-size scaling functions of the form $\Theta_\updownarrow(x_\updownarrow, \rho)$, with temperature scaling variable $x_\updownarrow \equiv (T/T_c - 1)(M/\xi^\updownarrow_0)^{1/\nu}$ and generalized aspect ratio $\rho \equiv (L/\xi^\leftrightarrow_0)/(M/\xi^\updownarrow_0)$, that only depend on the bulk and surface universality classes of the model [23, 24], as well as on the BCs. They have been calculated exactly for many cases, albeit mostly in strip geometry, where the aspect ratio ρ of the system goes to zero [25–31]. The theoretical results from exact calculations, field theory and Monte Carlo simulations [28–42] were shown to be in excellent agreement with experiments [43–50] for various bulk and surface universality classes.

Directly at the critical point, exact methods or conformal field theory [51–55] can be used to get exact expressions for the Casimir amplitude $\Delta_C(\rho)$ for arbitrary ρ. This has been done for periodic [56, 57] as well as for open BCs [58, 59]. Using conformal maps, these results can be used to investigate fluctuation-induced forces between colloids in critical suspensions both in theory [60–68] and experiment [69–77]. At arbitrary aspect ratios and temperatures, however, the finite-size scaling functions must be derived from the exact solution of the finite system with the correct BCs. For the Ising model, this has been done only in a few cases, namely for the torus with periodic BCs in both directions [22, 78, 79], for the cylinder with open or fixed at the boundaries in one direction [78, 80], and for the open rectangle considered here [11].

In this work, the calculations of [9] are substantially simplified by (i) the use of elliptic functions [5], (ii) a simplified normalization of the eigenvectors of the relevant $M \times M$ transfer matrices, (iii) a transformation to Hankel and Toeplitz matrices, and (iv) a representation of

[1] The relation '$\simeq$' denoted 'asymptotically equal' in the respective limit, and $\equiv$ denotes a definition.

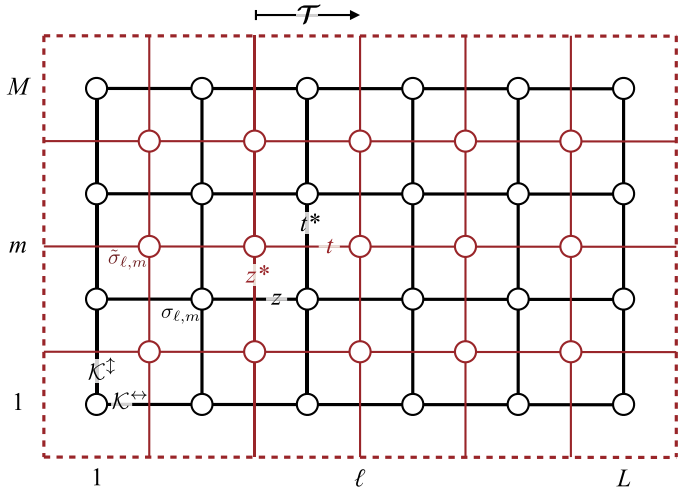

Figure 1. The anisotropic square lattice Ising model on the $L \times M$ rectangle (black), together with its dual lattice (red) and with the relevant couplings (see text). The transfer matrix $\mathcal{T}$ (1.6) propagates as indicated.

the sums over transfer matrix eigenvalues through a complex contour integral, having (v) a remarkably simple integrand given by the ratio of two very simple characteristic polynomials (CPs), each representing one direction of the two-dimensional Ising model. The preceding publication [9] will be denoted I in the following.

1.1. The model

This work focuses on the anisotropic square lattice Ising model on the $L \times M$ open rectangle, shown in figure 1. Our aim is to calculate the partition function

$$Z = \operatorname{tr} \exp\left(\mathcal{K}^{\leftrightarrow} \sum_{\ell=1}^{L-1} \sum_{m=1}^{M} \sigma_{\ell,m}\sigma_{\ell+1,m} + \mathcal{K}^{\updownarrow} \sum_{\ell=1}^{L} \sum_{m=1}^{M-1} \sigma_{\ell,m}\sigma_{\ell,m+1} \right), \tag{1.1}$$

with reduced couplings $\mathcal{K}^{\delta} = \beta J^{\delta}$ in direction $\delta = \leftrightarrow, \updownarrow$, where the trace is over all 2^{LM} configurations of the LM spins $\sigma_{\ell,m} = \pm 1$. We assume open BCs both in horizontal (L) and in vertical (M) directions, and we assume even M. The starting point of this work is the matrix product representation (I.29) of the well known Pfaffian representation by McCoy *et al* [4, 14], derived in [9] using a Schur reduction as well as a block transfer matrix formula by Molinari [17]. We follow the notation of [9], with a few clarifying minor modifications. Therefore, we define the dual

$$a^* \equiv \frac{1-a}{1+a} \tag{1.2}$$

of some quantity a, as well as the quite useful abbreviations[2]

$$a_{\pm} \equiv \frac{a \pm a^{-1}}{2} \tag{1.3}$$

[2] Subscripts $a_{\pm}$ are consequently used in this manner, while superscripts $a^{\pm}$ may have different meanings.

introduced in (I.20), fulfilling $(a^*)^* = a = a_+ + a_-$. The reduced couplings $\mathcal{K}^\delta$ are rewritten using the weights z and t according to

$$z \equiv \tanh \mathcal{K}^{\leftrightarrow}, \qquad t \equiv (\tanh \mathcal{K}^{\updownarrow})^* = \mathrm{e}^{-2\mathcal{K}^{\updownarrow}}. \tag{1.4}$$

The partition function Z of the considered anisotropic Ising model with open BCs in both directions is invariant under exchange of the two directions $\leftrightarrow$ and $\updownarrow$, where both the system dimensions and the coupling constants are exchanged according to the *swap transformation*

$$\mathcal{S} : (L, M; \mathcal{K}^{\leftrightarrow}, \mathcal{K}^{\updownarrow}) \mapsto \mathcal{S}[(L, M; \mathcal{K}^{\leftrightarrow}, \mathcal{K}^{\updownarrow})] = (M, L; \mathcal{K}^{\updownarrow}, \mathcal{K}^{\leftrightarrow}), \tag{1.5}$$

such that $Z = \mathcal{S}[Z]$. The swap transformation is an involution, as $\mathcal{S}[\mathcal{S}[a]] = a$. We now summarize the required results from reference [9].

1.2. Starting point

In equations (27)–(29) of [9] we showed that the square of the partition function (1.1) is proportional to the determinant of a matrix product of the form $\langle \mathbf{e}_2 | \boldsymbol{\mathcal{T}}_2^L | \mathbf{e}_2 \rangle$, with real hyperbolic 2×2 block transfer matrix $\boldsymbol{\mathcal{T}}_2$ propagating in horizontal direction. In this work, we will use a 'Wick rotated' version of $\boldsymbol{\mathcal{T}}_2$ according to[3] $\boldsymbol{\mathcal{T}} \equiv \boldsymbol{\mathcal{I}} \boldsymbol{\mathcal{T}}_2 \boldsymbol{\mathcal{I}}^\dagger$, with matrix $\boldsymbol{\mathcal{I}} \equiv \begin{pmatrix} 1 & 0 \\ 0 & \mathrm{i} \end{pmatrix} \otimes \mathbf{1}$, leading to the complex orthogonal block transfer matrix

$$\boldsymbol{\mathcal{T}} \equiv \begin{bmatrix} \mathbf{T}_+ & -\mathrm{i}\mathbf{T}_- \\ \mathrm{i}\mathbf{T}_- & \mathbf{T}_+ \end{bmatrix}, \tag{1.6}$$

which fulfills $\boldsymbol{\mathcal{T}}^{-1} = \boldsymbol{\mathcal{T}}^\top$. Note that $\boldsymbol{\mathcal{T}}$ is not unitary. The two real symmetric $M \times M$ matrices $\mathbf{T}_\pm$ were given in (I.30) and can be simplified to

$$\mathbf{T}_+ = -\frac{t_- z_-}{2} \underbrace{\begin{pmatrix} 2 + \frac{t^*}{z^*} & 1 & & & \\ 1 & 2 & \ddots & & \\ & \ddots & \ddots & \ddots & \\ & & \ddots & 2 & 1 \\ & & & 1 & 2 + t^* z^* \end{pmatrix}}_{\mathbf{C}} + (t_+ z_+ + t_- z_-)\mathbf{1}, \tag{1.7a}$$

$$\mathbf{T}_- = -\frac{t_- z_-}{2} \begin{pmatrix} & & & z^* & -\frac{1}{t^*} \\ & & \iddots & -2t^*_+ & \frac{1}{z^*} \\ & \iddots & \iddots & \iddots & \\ z^* & -2t^*_+ & \iddots & & \\ -\frac{1}{t^*} & \frac{1}{z^*} & & & \end{pmatrix}, \tag{1.7b}$$

[3] $\mathbf{A}^\top$ and $\mathbf{A}^\dagger$ denote the transpose and the conjugate transpose of $\mathbf{A}$, respectively.

using the dual couplings z^* and t^* (the matrix $\mathbf{C}$ will be utilized later). They are related via the transfer matrix $\mathbf{T} = \mathbf{T}_+ + \mathbf{T}_-$ according to (1.3),

$$\mathbf{T}_\pm = \frac{1}{2}\left(\mathbf{T} \pm \mathbf{T}^{-1}\right) \quad \Leftrightarrow \quad \mathbf{T}^{\pm 1} = \mathbf{T}_+ \pm \mathbf{T}_-, \tag{1.8}$$

from which directly follows that $\boldsymbol{\mathcal{T}}$ can be block diagonalized through a rotation by $\pi/4$,

$$\boldsymbol{\mathcal{R}}_{\frac{\pi}{4}}\boldsymbol{\mathcal{I}}^\dagger\boldsymbol{\mathcal{T}}\boldsymbol{\mathcal{I}}\boldsymbol{\mathcal{R}}_{-\frac{\pi}{4}} = \begin{bmatrix}\mathbf{T} & \mathbf{0}\\ \mathbf{0} & \mathbf{T}^{-1}\end{bmatrix}, \tag{1.9}$$

with block rotation matrix $\boldsymbol{\mathcal{R}}_\theta \equiv \begin{pmatrix}\cos\theta & \sin\theta\\ -\sin\theta & \cos\theta\end{pmatrix} \otimes \mathbf{1}$, for details see chapter 5 in [9]. The open BCs in horizontal direction are represented through the boundary state

$$|\mathbf{e}_\mathrm{o}\rangle \equiv \frac{1}{\sqrt{2}}|\mathbf{1} \quad \mathrm{i}\mathbf{S}\rangle, \quad \langle\mathbf{e}_\mathrm{o}|\mathbf{e}_\mathrm{o}\rangle = \mathbf{1}, \tag{1.10}$$

where $|\mathbf{e}_\mathrm{o}\rangle$ is a two element block vector, with the $M \times M$ matrices

$$\mathbf{1} \equiv \begin{pmatrix}1 & & \\ & \ddots & \\ & & 1\end{pmatrix}, \qquad \mathbf{S} \equiv \begin{pmatrix} & & 1\\ & \iddots & \\ 1 & & \end{pmatrix}. \tag{1.11}$$

Together with the constant

$$Z_0 \equiv (1-z^2)^{\frac{M}{2}}\left(\frac{2}{-z_-}\right)^{\frac{LM}{2}}, \tag{1.12}$$

the square of the partition function (1.1) then reads

$$Z^2 = Z_0^2 \det\langle\mathbf{e}_\mathrm{o}|\boldsymbol{\mathcal{T}}^L|\mathbf{e}_\mathrm{o}\rangle, \tag{1.13}$$

see also [7, (2.35)]. Defining the projectors

$$\mathbf{S}^\pm \equiv \frac{1}{2}\left(\mathbf{1} \pm \mathbf{S}\right), \tag{1.14}$$

the argument of the determinant in (1.13) becomes

$$\langle\mathbf{e}_\mathrm{o}|\boldsymbol{\mathcal{T}}^L|\mathbf{e}_\mathrm{o}\rangle = \langle\mathbf{S}^+ \quad \mathrm{i}\mathbf{S}^-|\begin{bmatrix}\mathbf{T}^L & \mathbf{0}\\ \mathbf{0} & \mathbf{T}^{-L}\end{bmatrix}|\mathbf{S}^+ \quad \mathrm{i}\mathbf{S}^-\rangle \tag{1.15a}$$

$$= \mathbf{S}^+\,\mathbf{T}^L\,\mathbf{S}^+ + \mathbf{S}^-\,\mathbf{T}^{-L}\,\mathbf{S}^- = M^\top\mathbf{M}, \tag{1.15b}$$

with the matrix

$$\mathbf{M} \equiv \mathbf{x}\left(\mathbf{T}^{L/2}\,\mathbf{S}^+ + \mathbf{T}^{-L/2}\,\mathbf{S}^-\right), \tag{1.16}$$

as $\mathbf{S}^+\mathbf{S}^- = \mathbf{0}$. In the following we will determine the eigenvalues $\lambda_\mu, \lambda_{\pm,\mu}$ and common eigenvectors $\vec{x}_\mu = (\mathbf{x})_\mu$ of $\mathbf{T}$ and $\mathbf{T}_\pm$, which fulfill

$$\mathbf{T}\,\vec{x}_\mu = \lambda_\mu\vec{x}_\mu, \qquad \mathbf{T}_\pm\vec{x}_\mu = \lambda_{\pm,\mu}\vec{x}_\mu, \tag{1.17}$$

where $\mu = 1, \ldots, M$.

1.3. The Onsager dispersion relation

The next step in the calculation of the partition function (1.1) is the determination of the eigenvalues $\lambda_{+,\mu}$ as zeroes of the characteristic polynomial (CP) of the tridiagonal matrix $\mathbf{T}_+$ from (1.7a), which will lead to the Onsager dispersion relation. As we will discuss several CPs in the following, we first define the CP $P_{\boldsymbol{a}}(x)$ of an arbitrary $M \times M$ matrix $\mathbf{A}$, with eigenvalues $(\boldsymbol{a})_\mu = a_\mu \in \mathbb{C}$, to be

$$P_{\boldsymbol{a}}(x) \equiv \det(x\mathbf{1} - \mathbf{A}) = \prod_{\mu=1}^{M} (x - a_\mu), \tag{1.18}$$

such that $P_{\boldsymbol{a}}(x)$ is a polynomial of degree M in the indeterminate $x \in \mathbb{C}$.

Using the well known recursion formula for tridiagonal matrices (see, e.g., [17]), in [9] we derived[4]

$$P_{\boldsymbol{\lambda}_+}(\lambda_+) = \det(\lambda_+\mathbf{1} - \mathbf{T}_+) = \prod_{\mu=1}^{M} (\lambda_+ - \lambda_{+,\mu}) \tag{1.19a}$$

$$= \left(\frac{t_- z_-}{2}\right)^M \langle\, 1/z^* \; -t^* \,|\, \mathbf{Q}^M \,|\, z^* \; t^* \,\rangle, \tag{1.19b}$$

where $\lambda_+ \in \mathbb{C}$. We point out the obvious similarity between equations (1.13) and (1.19b), which will become clearer later. The vertically propagating 2×2 transfer matrix

$$\mathbf{Q} \equiv \begin{pmatrix} 2\dfrac{t_+ z_+ - \lambda_+}{t_- z_-} & -1 \\ 1 & 0 \end{pmatrix} = \begin{pmatrix} 2\zeta_+ & -1 \\ 1 & 0 \end{pmatrix} = \begin{pmatrix} 2\cos\varphi & -1 \\ 1 & 0 \end{pmatrix} \tag{1.20}$$

has the eigenvalues $\zeta^{\pm 1}$ with modulus one[5], such that the nth power of $\mathbf{Q}$ reads

$$\mathbf{Q}^n = \frac{1}{\sin\varphi} \begin{pmatrix} \sin([n+1]\varphi) & -\sin(n\varphi) \\ \sin(n\varphi) & -\sin([n-1]\varphi) \end{pmatrix}. \tag{1.21}$$

Here and in the following, we express the horizontal and vertical eigenvalues (λ, ζ) through the introduced angles (γ, φ) according to

$$\lambda = \mathrm{e}^{\gamma}, \qquad \lambda_+ = \cosh\gamma, \qquad \lambda_- = \sinh\gamma, \tag{1.22a}$$

$$\zeta = \mathrm{e}^{\mathrm{i}\varphi}, \qquad \zeta_+ = \cos\varphi, \qquad \zeta_- = \mathrm{i}\sin\varphi. \tag{1.22b}$$

Equation (1.20) is the point in the calculation where the famous Onsager dispersion relation

$$\lambda_+ + t_- z_- \zeta_+ = t_+ z_+ \quad \Leftrightarrow \quad \cosh\gamma + t_- z_- \cos\varphi = t_+ z_+ \tag{1.23}$$

between the eigenvalues λ and ζ enters the stage, which plays the key role in the exact solution of the square lattice Ising model [2]. It relates the two 'good' variables λ and ζ for propagation in $\leftrightarrow$ (L) and $\updownarrow$ (M) direction, respectively. As pointed out by Baxter [5, chapter 15.10], a

[4] The sign change in the definition w.r.t. (I.9) has no effect for even M.

[5] $\zeta^{\pm 1}$ were denoted $q^{\pm}$ in (I.42).

parametrization of relation (1.23) using elliptic functions considerably simplifies the analysis. This parametrization is introduced in the next chapter, and we return to the CPs in section 3.1.

2. Elliptic parametrization

The key idea behind the elliptic parametrization of the Onsager dispersion relation (1.23) is (i) to substitute the coupling constants (z, t) through new constants (k, η), where k is temperature-like and η encodes the coupling anisotropy, and (ii) to introduce a complex variable u that simultaneously parametrizes the quantities $\zeta = \zeta(u)$ and $\lambda = \lambda(u)$ in such a way that (1.23) is always fulfilled[6]. We recapitulate the parametrization of (1.23) through the Jacobi elliptic functions $\mathrm{sn}(u, k)$, $\mathrm{cn}(u, k)$ and $\mathrm{dn}(u, k)$ [81–83], with elliptic modulus k, by first defining the Jacobi amplitude

$$\phi \equiv \mathrm{am}(u, k) \tag{2.1}$$

as the inverse function of the elliptic integral of the first kind

$$u = F(\phi, k) \equiv \int_0^\phi (1 - k^2 \sin^2\theta)^{-1/2} \mathrm{d}\theta, \tag{2.2}$$

for $\{\phi, u, k\} \in \mathbb{R}$. Consequently, the Jacobi elliptic functions are given by

$$\mathrm{sn}(u, k) \equiv \sin\,\phi, \quad \mathrm{cn}(u, k) \equiv \cos\,\phi, \quad \mathrm{dn}(u, k) \equiv \frac{\partial\phi}{\partial u} = \pm\sqrt{1 - k^2 \sin^2\phi}, \tag{2.3}$$

and fulfill the sum of squares identities

$$\mathrm{sn}^2(u, k) + \mathrm{cn}^2(u, k) = k^2\,\mathrm{sn}^2(u, k) + \mathrm{dn}^2(u, k) = 1. \tag{2.4}$$

As common, we suppress the modulus k if possible and write, e.g., $\mathrm{sn}\,u$ instead of $\mathrm{sn}(u, k)$. We follow Glashier's notation [83, (22.2.10)] and define all sixteen Jacobi elliptic functions

$$\mathrm{pq}\,u \equiv \frac{\mathrm{pr}\,u}{\mathrm{qr}\,u} = \frac{1}{\mathrm{qp}\,u}, \qquad \text{where } \mathrm{p}, \mathrm{q}, \mathrm{r} \in \{\mathrm{s}, \mathrm{c}, \mathrm{d}, \mathrm{n}\}, \tag{2.5}$$

including the four trivial ones, $\mathrm{ss}\,u = \mathrm{cc}\,u = \mathrm{dd}\,u = \mathrm{nn}\,u = 1$.

The Jacobi elliptic functions are double periodic and meromorphic in the complex u-plane, that is they are analytic up to simple poles. The common quarter-periodicity rectangle has the corners

$$\{u_\mathrm{s}, u_\mathrm{c}, u_\mathrm{d}, u_\mathrm{n}\} \equiv \{0, K, K + \mathrm{i}K', \mathrm{i}K'\}, \tag{2.6}$$

see figure 2, where we utilized the graphical interpretation from [83, (22.4)] and associate the denomination $\{\mathrm{s}, \mathrm{c}, \mathrm{d}, \mathrm{n}\}$ with the four vertices of the quarter-periodicity rectangle. Eventually, the quarter periods K and K' are the complete elliptic integrals of the first kind,

$$K \equiv F\left(\frac{\pi}{2}, k\right), \qquad K' \equiv F\left(\frac{\pi}{2}, k'\right), \tag{2.7}$$

[6] Imagine the simpler case of a circle $x^2 + y^2 = r^2$ being trigonometrically parametrized, with $x(u) = r\cos u$, $y(u) = r\sin u$ and complex parameter u.

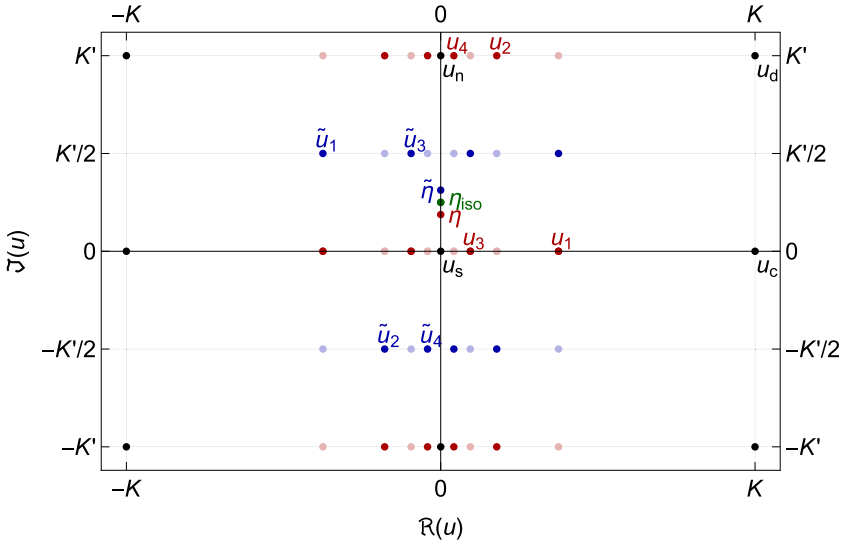

Figure 2. Structure of the complex elliptic u-plane for $M = 4$, paramagnetic temperature $k = 0.95$, and anisotropy $\eta = \frac{3}{4}\eta_{\mathrm{iso}}$. The eigenvalues λ_μ translate to the points u_μ (red), while the swap-transformed points $\tilde{u}_\mu$ (blue) represent the eigenvalues ζ_μ and lie point-symmetric w.r.t. the point η_{iso} (green) from (2.15). The corners (2.6) of the quarter-periodicity rectangle are shown in black. The additional eigenvalues λ_μ^{-1} at positions $\check{u}_\mu \equiv u_\mu + \mathrm{i}K'$ (C.5) and the corresponding eigenvalues ζ_μ^{-1} are shown in light colors.

cf (2.2), with complementary modulus k' fulfilling $k^2 + k'^2 = 1$. This elliptic parametrization will lead to substantial simplifications of the results from [9], as it firstly eliminates the sign ambiguities of the square roots and secondly introduces certain functions of the parameter u that substantially simplify the expressions.

2.1. Coupling constants parametrization

There are several possible ways to setup an elliptic parametrization of the Onsager dispersion relation (1.23): one could set $k = \hat{k} \equiv z_-/t_-$ such that $0 \leqslant \hat{k} < 1$ holds in the ordered phase. This choice is usually used in the literature [7, 84]. However, we will argue that many expressions become considerably simpler if we instead use the modulus

$$k \equiv \frac{t_-}{z_-}, \tag{2.8}$$

being the reciprocal of $\hat{k}$. It obeys $0 \leqslant k < 1$ in the disordered phase $T > T_\mathrm{c}$ and $k > 1$ in the ordered phase $T < T_\mathrm{c}$, similar to the reduced inverse temperature β/β_c. Note that K becomes complex for $k > 1$, and we can replace it with its real part, $K \mapsto \Re(K) = K + \mathrm{i}K'$, in the complex analysis in order to keep an un-tilted quarter-periodicity rectangle.

The anisotropy parameter η can be introduced in several ways, too. We choose the definition

$$\mathrm{sn}(2\eta) \equiv \frac{1}{\mathrm{i}t_-}, \tag{2.9}$$

such that η is a purely imaginary point in the u-plane, with $0 \leqslant \Im(\eta) \leqslant K'/2$. This leads to the identities

$$t = \frac{\operatorname{sn}\eta \operatorname{dn}\eta}{\mathrm{i}\operatorname{cn}\eta}, \qquad t_+ = \mathrm{i}\operatorname{cs}(2\eta), \qquad t_- = \frac{1}{\mathrm{i}}\operatorname{ns}(2\eta), \tag{2.10a}$$

$$z = k\frac{\operatorname{sn}\eta \operatorname{cn}\eta}{\mathrm{i}\operatorname{dn}\eta}, \qquad z_+ = \frac{\mathrm{i}}{k}\operatorname{ds}(2\eta), \qquad z_- = \frac{1}{\mathrm{i}k}\operatorname{ns}(2\eta). \tag{2.10b}$$

For the dual couplings we find the corresponding expressions

$$t^*_+ = -\frac{t_+}{t_-} = \operatorname{cn}(2\eta), \qquad t^*_- = \frac{1}{t_-} = \mathrm{i}\operatorname{sn}(2\eta), \tag{2.11a}$$

$$z^*_+ = -\frac{z_+}{z_-} = \operatorname{dn}(2\eta), \qquad z^*_- = \frac{1}{z_-} = \mathrm{i}k\operatorname{sn}(2\eta), \tag{2.11b}$$

which implies that we can express t, z, t^* and z^* through the Jacobi amplitude (2.1),

$$t^* = \mathrm{e}^{\mathrm{i}\operatorname{am}(2\eta)}, \qquad t = -\mathrm{i}\tan\left[\frac{1}{2}\operatorname{am}(2\eta)\right], \tag{2.12a}$$

$$z = \mathrm{e}^{\mathrm{i}\operatorname{am}(2\tilde{\eta})}, \qquad z^* = -\mathrm{i}\tan\left[\frac{1}{2}\operatorname{am}(2\tilde{\eta})\right], \tag{2.12b}$$

where $\tilde{u}$ denotes the swap transform (1.5) of a point u in the complex u-plane,

$$u \mapsto \tilde{u} \equiv \mathcal{S}(u) = \frac{1}{2}\mathrm{i}K' - u. \tag{2.13}$$

From (2.2) and the t^* identity (2.12a) we conclude that

$$2\eta = F(-\mathrm{i}\log t^*, k) = \mathrm{i}K' - F(-\mathrm{i}\log z, k). \tag{2.14}$$

Note that in the isotropic case $t^* = z$ the point η lies symmetrically at

$$\eta_{\mathrm{iso}} \equiv \frac{1}{4}\mathrm{i}K' = \tilde{\eta}_{\mathrm{iso}}, \tag{2.15}$$

as $\mathcal{S}(\eta_{\mathrm{iso}}) = \eta_{\mathrm{iso}}$. Therefore, the transformation (2.13) is a point reflection of the complex u-plane at the point η_{iso}.

2.2. Eigenvalues parametrization

The relation of the eigenvalues λ and ζ (1.22) to u is also ambiguous. We follow the literature [5, 7, 84] and define

$$\frac{1}{\sqrt{\lambda\zeta^{\pm 1}}} = \mathrm{e}^{-\frac{\gamma \pm \mathrm{i}\varphi}{2}} \equiv \sqrt{k}\operatorname{sn}(u \mp \eta), \tag{2.16}$$

such that

$$\lambda = \mathrm{e}^{\gamma} = \frac{1}{k\operatorname{sn}(u+\eta)\operatorname{sn}(u-\eta)}, \qquad \zeta = \mathrm{e}^{\mathrm{i}\varphi} = \frac{\operatorname{sn}(u+\eta)}{\operatorname{sn}(u-\eta)}. \tag{2.17}$$

The real and positive eigenvalues λ_μ correspond to values u_μ on the real axis (for $\lambda_\mu > 1$) as well as on the line $\Im(u_\mu) = \mathrm{i}K'$ (for $\lambda_\mu < 1$). With this definition of λ, the constants u_{p} and λ_{p}

from (2.6) and (A.1) fulfill $\lambda_\mathrm{p} = \lambda(u_\mathrm{p})$ and represent the upper and lower bound of the spectrum of $\mathbf{T}$ and $\mathbf{T}^{-1}$ both above and below T_c. In appendix A we give a subset of the large number of identities which can be derived using elliptic functions identities [81, 83]. Especially, we see from (A.11) that the eigenvalues λ and ζ are exchanged under the transformation $\mathcal{S}$ according to $\mathcal{S}[(\lambda,\zeta)] = (\zeta,\lambda)$.

Besides the corners of the quarter-periodicity rectangle (2.6), and the eigenvalues u_μ, where the CP (1.19) is zero, there are four other important points in the complex u-plane, namely the positions of the simple poles and simple zeroes of $\lambda(u)$ and $\zeta(u)$. Because the Jacobi $\mathrm{sn}\,u$ has a simple zero at $u = 0$ and a simple pole at $u = \mathrm{i}K'$, we find

$$u_{\lambda\to\infty,\zeta\to\infty} = +\eta, \qquad u_{\lambda\to0,\zeta\to\infty} = +\mathrm{i}K' - \eta, \tag{2.18a}$$

$$u_{\lambda\to\infty,\zeta\to0} = -\eta, \qquad u_{\lambda\to0,\zeta\to0} = -\mathrm{i}K' + \eta. \tag{2.18b}$$

These four points will be used later in the analysis of the complex structure of the relevant integrals.

While K and K' are the quarter periods of the Jacobi elliptic functions (2.3), all relevant parameters and variables of the considered system, such as t, z, λ, ζ, can be written as meromorphic functions of $2u$ and 2η, see (2.12), (A.16), and (A.17). They are therefore double periodic functions with quarter periods $K/2$ and $K'/2$ and *half periods* K and K', and can be depicted on the periodicity rectangle going from $-K - \mathrm{i}K'$ to $K + \mathrm{i}K'$, as shown in figure 2.

Finally, we remark that the CP zeroes show up in pairs $(u_\mu, -\bar{u}_\mu)$, lying symmetrically with respect to the imaginary axis, see figure 2. The reason for this symmetry is the meromorphicity of the Jacobi elliptic functions, and consequently of $\lambda(u)$ and $\zeta(u)$ from (2.17), in combination with the fact that both λ and ζ are real for purely imaginary u. Therefore, λ and ζ transform according to $f(u) = \overline{f(-\overline{u})}$ under conjugation. This symmetry is sometimes called *para-even* in the literature, and $-\bar{u}$ is denoted the *para-conjugate* of u [85, 6.29]. We could restore the usual symmetry along the real axis $f(u) = \overline{f(\overline{u})}$, valid for meromorphic functions $f(u)$ that are real for real u, by rotating the complex plane by 90° using the Jacobi imaginary transform [83, section 22.6(iv)]. This would however break the simple relation to the Jacobi amplitude introduced in the next section. Alternatively, one could also replace u by $\mathrm{i}u$ in all expressions as done in [5], but we will keep the present definition.

2.3. The Jacobi amplitudes ω and θ

It turns out in the next chapter that the Jacobi amplitude ω of $2u$, as well as its imaginary swap transform θ,

$$\omega \equiv \mathrm{am}(2u), \qquad \theta \equiv \mathrm{i}\,\mathrm{am}(2\tilde{u}), \tag{2.19}$$

with $\tilde{u}$ from (2.13), will play quite important roles in the following[7]. They satisfy the identities

$$\mathrm{sn}(2u) = \sin\,\omega, \qquad \mathrm{sn}(2\tilde{u}) = \frac{1}{\mathrm{i}}\,\sinh\,\theta = -\frac{1}{k}\,\mathrm{ns}(2u), \tag{2.20a}$$

$$\mathrm{cn}(2u) = \cos\,\omega, \qquad \mathrm{cn}(2\tilde{u}) = \cosh\,\theta = \frac{\mathrm{i}}{k}\,\mathrm{ds}(2u), \tag{2.20b}$$

$$\mathrm{dn}(2u) = -\coth\,\theta = \mathrm{i}\,\mathrm{cs}(2\tilde{u}), \qquad \mathrm{dn}(2\tilde{u}) = \mathrm{i}\,\cot\,\omega = \mathrm{i}\,\mathrm{cs}(2u), \tag{2.20c}$$

[7] Note that *Mathematica* [86] can correctly handle the complex Jacobi amplitude only since version 12.1.

as well as

$$\tan\left(\frac{1}{2}\omega\right) = \frac{\mathrm{sn\,u\,dn\,u}}{\mathrm{cn\,u}}, \qquad \mathrm{e}^{\pm\theta} = \left(k\frac{\mathrm{sn\,u\,cn\,u}}{\mathrm{i\,dn\,u}}\right)^{\pm 1}, \tag{2.21}$$

and fulfill the symmetric relation

$$\mathrm{i}k\,\sin\,\omega\,\sinh\,\theta = 1. \tag{2.22}$$

In summary, we have defined a double periodic complex manifold with the topology of a torus as originally proposed by Baxter [5], to describe the two-dimensional Ising model on the rectangle. This complex manifold will be called the u-plane and is sketched in figure 2. The aspect ratio of the torus is temperature-dependent and is encoded in the elliptic modulus k, while the coupling anisotropy is described by a point η on the torus. The M eigenvalues λ_μ and ζ_μ correspond to points u_μ and $\tilde{u}_\mu$, respectively, on the torus. With this set of definitions, we now can return to the CP from section 1.3.

3. Results

3.1. Characteristic polynomials

The CP $P_{\boldsymbol{\lambda}_+}(\lambda_+)$ of the matrix $\mathbf{T}_+$ was defined in chapter 6 of [9]. It was used to characterize the spectrum of $\mathbf{T}_+$ and to derive the finite-size scaling limit in [11]. For the transfer matrix $\mathbf{T}_+$ with eigenvalues $\lambda_{+,\mu}$, equation (1.19b) can be simplified to

$$P_{\boldsymbol{\lambda}_+}(\lambda_+) = (1-t^{*2})\left(\frac{t_- z_-}{2}\right)^M \left[\cos(M\varphi) + \frac{t_+ z_- \,\cos\,\varphi - t_- z_+}{z_-\,\sin\,\varphi}\,\sin(M\varphi)\right], \tag{3.1}$$

cf (I.45), where the angle[8] φ is given by the Onsager dispersion relation (1.23). Using the elliptic parametrization from the last section, and especially the Jacobi amplitude ω from (2.19), we find, using (2.10) and (A.17), the surprisingly simple expressions

$$P_{\boldsymbol{\lambda}_+}(\lambda_+) = (1-t^{*2})\left(\frac{t_- z_-}{2}\right)^M [\cos(M\varphi) - cs(2u)\sin(M\varphi)] \tag{3.2a}$$

$$= (1-t^{*2})\left(\frac{t_- z_-}{2}\right)^M \frac{\sin(M\varphi-\omega)}{\sin(-\omega)}, \tag{3.2b}$$

as $\mathrm{cs}(2u) = \cot\omega$ by (2.20c). Here, λ_+ and φ depend on u according to (2.17), (A.11a), or (A.16) and (A.17). As a consequence, the eigenvalues $\lambda_{+,\mu}$ of $\mathbf{T}_+$ fulfill the simple condition $M\varphi_\mu = \omega_\mu$. These simplifications demonstrate the power of the elliptic parametrization in the chosen form, and the introduced Jacobi amplitude ω (2.19) turns out to be a phase shift in φ-space, describing the open BCs in $\updownarrow$ direction.

Due to the linear CP identity

$$P_{c\boldsymbol{a}+b}(cx+b) = \prod_{\mu=1}^{M}(cx+b-ca_\mu-b) = c^M P_{\boldsymbol{a}}(x), \tag{3.3}$$

[8] For the correct determination of the sign of φ without elliptic parametrization, see chapter 6 in [9].

we can rewrite (3.2b) in terms of the new variable

$$\chi \equiv 2(\zeta_+ + 1) = 4\cos^2\left(\frac{1}{2}\varphi\right) = \frac{2}{t_- z_-}(t_+ z_+ + t_- z_- - \lambda_+), \tag{3.4}$$

eliminating the factor $(t_- z_-/2)^M$, and find the corresponding CP

$$P_\chi(\chi) = (1 - t^{*2})\,\frac{\sin(M\varphi - \omega)}{\sin(-\omega)}. \tag{3.5}$$

Comparing (3.4) and (1.7a), we see that $P_\chi(\chi)$ is the CP of the matrix $\mathbf{C}$, which therefore has the eigenvalues χ_μ.

3.2. Common eigenvectors

With the help of the introduced elliptic parametrization, the matrix $\mathbf{x}$ of orthonormal common eigenvectors[9] of $\mathbf{T}_\pm$, $\mathbf{T}$ and $\mathbf{C}$, defined in (1.17) and originally given in (I.50), can be considerably simplified, too. Using the projectors $\mathbf{S}^\pm$ from (1.14), we can split $\mathbf{x}$ into an even part $\mathbf{x}^+$ and an odd part $\mathbf{x}^-$ according to $\mathbf{x}^\pm \equiv \mathbf{x}\mathbf{S}^\pm$, such that $\mathbf{x} = \mathbf{x}^+ + \mathbf{x}^-$ and $\mathbf{x}^\pm = \pm\mathbf{x}^\pm\mathbf{S}$, i.e., $\mathbf{x}^+$ ($\mathbf{x}^-$) contains the symmetric (skew-symmetric) parts of the eigenvectors. We get

$$\mathbf{x}^+ = \frac{1}{\sqrt{2}}\mathbf{D}^{\frac{1}{2}}\left[\mathrm{e}^{-\frac{1}{2}\left(\theta_\mu - \psi_\mu + \frac{\mathrm{i}\pi}{2}\right)}\,\frac{\cos\left(\frac{m}{2}\varphi_\mu\right)}{\cos\left(\frac{1}{2}\varphi_\mu\right)}\right]^M_{\mu=1,\,m\text{ odd}}, \tag{3.6a}$$

$$\mathbf{x}^- = \frac{1}{\sqrt{2}}\mathbf{D}^{\frac{1}{2}}\left[\mathrm{e}^{+\frac{1}{2}\left(\theta_\mu - \psi_\mu + \frac{\mathrm{i}\pi}{2}\right)}\,\frac{\sin\left(\frac{m}{2}\varphi_\mu\right)}{\sin\left(\frac{1}{2}\varphi_\mu\right)}\right]^M_{\mu=1,\,m\text{ odd}}, \tag{3.6b}$$

where m runs over the odd integers between $-M$ and M. The angle ψ is defined through

$$\mathrm{e}^{\frac{1}{2}(\theta-\psi)} \equiv \sqrt{\mathrm{i}z}\,\frac{\mathrm{cn}\,u}{\mathrm{cn}\,\eta}, \tag{3.7}$$

with θ from (2.19), cf (2.21) and (A.12c), and fulfills

$$\mathrm{e}^{-\psi} = -\mathrm{i}\zeta^* = -\tan\left(\frac{1}{2}\varphi\right), \tag{3.8}$$

see also (D.3b). Using the CP $P_{\lambda_+}(\lambda_+)$ from (3.2), or alternatively $P_\chi(\chi)$ from (3.5), the diagonal normalization matrix $\mathbf{D}$ can be substantially simplified from the expression given in (I.50), with the result

$$(\mathbf{D})_{\mu\mu} = -\frac{t^*}{z_-}\left(\frac{t_- z_-}{2}\right)^{M-1}\frac{1}{P'_{\lambda_+}(\lambda_{+,\mu})} \tag{3.9a}$$

$$= \frac{t^*}{z_-}\frac{1}{P'_\chi(\chi_\mu)}. \tag{3.9b}$$

Here we used a relation between the normalization of the eigenvectors of a tridiagonal matrix and the derivative P' of its CP [87, chapter 7.9]. With these simplifications and the diagonal eigenvalue matrix $(\mathbf{\Lambda})_{\mu\mu} = \lambda_\mu$, we can rewrite (1.16) as

$$\mathbf{M} = \mathbf{\Lambda}^{L/2}\,\mathbf{x}^+ + \mathbf{\Lambda}^{-L/2}\,\mathbf{x}^-, \tag{3.10}$$

[9] The eigenvectors $\vec{x}_\mu$ are row vectors in $\mathbf{x}$, i.e., $\vec{x}_\mu = (\mathbf{x})_\mu$.

and the partition function (1.13) becomes $Z = Z_0 \det \mathbf{M}$. Inserting the definition of $\mathbf{x}^{\pm}$ into (3.10), we get the result

$$\hat{\mathbf{W}} \equiv \frac{1}{\sqrt{2}} \left[\mathrm{e}^{\frac{1}{2}\left(L\gamma_\mu - \theta_\mu + \psi_\mu - \frac{\mathrm{i}\pi}{2}\right)} \frac{\cos\left(\frac{m}{2}\varphi_\mu\right)}{\cos\left(\frac{1}{2}\varphi_\mu\right)} + \mathrm{e}^{-\frac{1}{2}\left(L\gamma_\mu - \theta_\mu + \psi_\mu - \frac{\mathrm{i}\pi}{2}\right)} \frac{\sin\left(\frac{m}{2}\varphi_\mu\right)}{\sin\left(\frac{1}{2}\varphi_\mu\right)} \right]^M_{\mu=1,\, m\,\mathrm{odd}}, \tag{3.11}$$

such that (1.15) becomes $\mathbf{M}^\top \mathbf{M} = \hat{\mathbf{W}}^\top \mathbf{D} \hat{\mathbf{W}}$.

As shown in [9], the matrix $\hat{\mathbf{W}}$ is a generalized Vandermonde matrix, such that a change of the base leaves the value of the determinant invariant. Hence we can transform from the trigonometric base to the simpler power base and get the corresponding matrix

$$\mathbf{W} \equiv \left[\mathrm{e}^{H(m)(L\gamma_\mu - \theta_\mu + \psi_\mu)}\, \chi_\mu^{\frac{1}{2}(|m|-1)} \right]^M_{\mu=1,\, m\,\mathrm{odd}}, \tag{3.12}$$

with the Heaviside step function H, where we have used the variable χ introduced in (3.4), and factored out the exponential for $m < 0$ and moved it to the diagonal matrix

$$\mathbf{F} \equiv \left[\delta_{\mu\nu}\, \mathrm{e}^{-\frac{1}{2}(L\gamma_\mu - \theta_\mu + \psi_\mu)} \right]^M_{\mu,\nu=1}, \tag{3.13}$$

such that $\det \hat{\mathbf{W}} = \det \mathbf{F} \det \mathbf{W}$. As $\det \mathbf{F} = t^{-\frac{L}{2}}$ by (3.7), (D.1a) and (D.3b), the resulting squared partition function now reads

$$Z^2 = Z_0^2\, t^{-L} \det(\mathbf{W}^\top \mathbf{D} \mathbf{W}). \tag{3.14}$$

Up to here, the calculation was similar to [9], with one major difference: the occurrence of the terms $1/P'_{\boldsymbol{\chi}}(\chi_\mu)$ in the diagonal matrix $\mathbf{D}$ (3.9b) will enable us to use a relation between CPs, their associated Vandermonde matrices and certain Hankel matrices.

3.3. Hankelization

The next significant simplification is obtained by utilizing a generalization of the well known relation of the CP $P_{\boldsymbol{x}}(x)$ and the related Vandermonde matrix

$$\mathbf{V}_{\boldsymbol{x}} \equiv \left[x_\mu^j \right]^{M \quad M-1}_{\mu=1,\; j=0} \tag{3.15}$$

to a certain Hankel matrix $\mathbf{H}_{\boldsymbol{x}}$ [88, 89], also known as 'Vandermonde factorization of a Hankel matrix'. Let

$$P_{\boldsymbol{x}}(x) = \prod_{\mu=1}^{M} (x - x_\mu) = \sum_{n=0}^{M} b_n x^n, \tag{3.16}$$

where $b_M = 1$ by construction, as well as

$$\mathbf{D}_{\boldsymbol{x}} \equiv \left[\frac{\delta_{\mu\nu}}{P'_{\boldsymbol{x}}(x_\mu)} \right]^M_{\mu,\nu=1}, \qquad \mathbf{H}_{\boldsymbol{x}}^{-1} \equiv \left[b_{i+j+1} \right]^{M-1}_{i,j=0}, \tag{3.17}$$

then

$$\mathbf{V}_{\boldsymbol{x}}^\top\, \mathbf{D}_{\boldsymbol{x}} \mathbf{V}_{\boldsymbol{x}} = \mathbf{H}_{\boldsymbol{x}}, \qquad \det{}^2 \mathbf{V}_{\boldsymbol{x}} \det \mathbf{D}_{\boldsymbol{x}} = 1. \tag{3.18}$$

While $\mathbf{H}_{\boldsymbol{x}}^{-1}$ is upper anti-triangular, $\mathbf{H}_{\boldsymbol{x}}$ itself is lower anti-triangular, e.g. for $M = 4$,

$$\mathbf{H}_{\boldsymbol{x}}^{-1} = \begin{pmatrix} b_1 & b_2 & b_3 & 1 \\ b_2 & b_3 & 1 & 0 \\ b_3 & 1 & 0 & 0 \\ 1 & 0 & 0 & 0 \end{pmatrix} \quad \Rightarrow \quad \mathbf{H}_{\boldsymbol{x}} = \begin{pmatrix} 0 & 0 & 0 & 1 \\ 0 & 0 & 1 & \tilde{b}_5 \\ 0 & 1 & \tilde{b}_5 & \tilde{b}_6 \\ 1 & \tilde{b}_5 & \tilde{b}_6 & \tilde{b}_7 \end{pmatrix}, \tag{3.19}$$

with[10] $\tilde{b}_n = \sum_\mu x_\mu^{n-1} / P'_{\boldsymbol{x}}(x_\mu)$.

A direct computation (see appendix B) shows that a similar identity holds for the generalized Vandermonde matrix $\mathbf{W}$ (3.12) in conjunction with $\mathbf{D}$ from (3.9b), namely

$$\mathbf{W}^\top \mathbf{D} \mathbf{W} = \begin{bmatrix} \mathbf{0} & \mathbf{S}\hat{\mathbf{H}}_1 \\ \hat{\mathbf{H}}_1 \mathbf{S} & \hat{\mathbf{H}}_2 \end{bmatrix} \tag{3.20}$$

with the $M/2 \times M/2$ Hankel matrices

$$\hat{\mathbf{H}}_\Delta \equiv \left[\sum_{\mu=1}^{M} \frac{t^*}{z_-} \frac{\mathrm{e}^{\Delta(L\gamma_\mu - \theta_\mu + \psi_\mu)}}{P'_\chi(\chi_\mu)} \chi_\mu^{i+j} \right]_{i,j=0}^{\frac{M}{2}-1}. \tag{3.21}$$

Note that (3.20) is block lower anti-triangular similar to $\mathbf{H}_{\boldsymbol{x}}$ in (3.19), as $\hat{\mathbf{H}}_0 = \mathbf{0}$. The important consequence of this result is the generalized determinant identity

$$\det(\mathbf{W}^\top \mathbf{D} \mathbf{W}) = \det{}^2 \mathbf{W} \ \det \mathbf{D} = \det{}^2 \hat{\mathbf{H}}_1, \tag{3.22}$$

which leads to the surprising result that the Ising partition function can be mapped to a Hankel determinant. Inserting the simplifications from above, and defining $\mathbf{H} \equiv 2\mathrm{i} z_- \hat{\mathbf{H}}_1$, we can draw the square root in (3.14) and get the compact exact expression for the partition function of the square lattice Ising model on the rectangle,

$$Z = Z_1 \ \det \mathbf{H}, \quad Z_1 \equiv t^{-\frac{L}{2}} z^{\frac{M}{2}} \left(-\frac{2}{z_-} \right)^{\frac{LM}{2}}, \tag{3.23a}$$

where the $M/2 \times M/2$ Hankel matrix $\mathbf{H} = \left[h_{i+j+1} \right]_{i,j=0}^{M/2-1}$ has the matrix elements

$$h_n \equiv \sum_{\mu=1}^{M} \frac{2\mathrm{i} t^* \, \mathrm{e}^{L\gamma_\mu - \theta_\mu + \psi_\mu}}{P'_\chi(\chi_\mu)} \chi_\mu^{n-1}, \tag{3.23b}$$

with $n = 1, \ldots, M-1$. This expression represents a significant simplification with respect to the result from [9]. However, in the next section we will proceed further by rewriting the sum over μ as a complex contour integral, inserting the known formula for $P_\chi(\chi)$ from (3.5).

3.4. Contour integral representation

The matrix elements h_n of the Hankel matrix $\mathbf{H}$ (3.23b) can be evaluated using complex contour integration, and the CP $P_\chi(\chi)$ plays a crucial role in this calculation. In principle we use

[10] As a side note, both $\tilde{b}_n = s_{(n-M)}(\boldsymbol{x})$ and $b_n = (-1)^n s_{\mathbf{1}_{M-n}}(\boldsymbol{x})$ are Schur polynomials.

Cauchy's residual theorem and calculate the sum over μ in h_n as a contour integral over a suitable contour C around the points u_μ in the complex u-plane,

$$h_n = \frac{1}{2\pi \mathrm{i}} \oint_C \frac{2\mathrm{i}t^* \, \mathrm{e}^{L\gamma-\theta+\psi}}{P'_\chi(\chi)} \, \chi^{n-1} \, \frac{\partial \, \log \, P_\chi(\chi)}{\partial \chi} \frac{\partial \chi}{\partial u} \, \mathrm{d}u \tag{3.24a}$$

$$= \frac{1}{2\pi \mathrm{i}} \oint_C \frac{2\mathrm{i}t^* \, \mathrm{e}^{L\gamma-\theta+\psi}}{P_\chi(\chi)} \, \chi^{n-1} \, \frac{\partial \chi}{\partial u} \, \mathrm{d}u, \tag{3.24b}$$

where, most importantly, the derivative $P'_\chi(\chi)$ cancels out.

While the CP $P_\chi(\chi)$ has two sets of zeroes u_μ and $\breve{u}_\mu$ corresponding to the eigenvalues λ_μ and λ_μ^{-1}, cf (C.5), the contour C only encloses the zeroes u_μ, see figure 2. We can easily remove the additional zeroes $\breve{u}_\mu$ by employing a factorization analog to (C.2),

$$P_\chi(\chi) = \frac{1 - t^{*2}}{2\mathrm{i} \, \sin \, \omega} \left[1 - \mathrm{e}^{\mathrm{i}(M\varphi-\omega)}\right] \left[1 + \mathrm{e}^{-\mathrm{i}(M\varphi-\omega)}\right]. \tag{3.25}$$

As the first (second) bracket vanishes at u_μ ($\breve{u}_\mu$), we can drop the additional zeroes $\breve{u}_\mu$ by replacing the last term with its value at the zeroes u_μ, where $M\varphi - \omega = 0$, to get

$$h_n = \frac{1}{2\pi \mathrm{i}} \oint_C \frac{\mathrm{e}^{L\gamma-\theta+\psi}}{1 - \mathrm{e}^{\mathrm{i}(M\varphi-\omega)}} \, t_- \, \sin \, \omega \, \chi^{n-1} \, \frac{\partial \chi}{\partial u} \, \mathrm{d}u. \tag{3.26}$$

In the next step we use (3.8), (A.19b) and (A.20) to eliminate ψ and $\sin\omega$. Furthermore, we can move the zeroes of the numerator to the line $\Im(u) = \frac{1}{2}K'$ without changing the integral by adding one to the numerator, such that the numerator $1 - \mathrm{e}^{L\gamma-\theta} = \mathcal{S}[1 - \mathrm{e}^{\mathrm{i}(M\varphi-\omega)}]$ is precisely the swap transform (1.5) of the denominator, with the result

$$h_n = \frac{1}{2\pi \mathrm{i}} \oint_C \frac{1 - \mathrm{e}^{L\gamma-\theta}}{1 - \mathrm{e}^{\mathrm{i}(M\varphi-\omega)}} \, \chi^n \, \frac{\partial \gamma}{\partial u} \, \mathrm{d}u. \tag{3.27}$$

Due to the CP property (3.3) and the Vandermonde property of (3.11), the determinant of (3.26) is invariant under a translation $\chi \mapsto \chi + c$. This freedom is used in (3.27), as χ was defined in (3.4) in order to obey $\chi = 2 \, \cot(\frac{1}{2}\varphi) \sin \, \varphi$.

The resulting integrand is shown in figure 3. At the four points $\{u_{0,\infty}, u_{\infty,\infty}, u_{\infty,0}, u_{0,0}\}$ (2.18) (black dots), the pole orders[11] $\{n+1-M, n+1+L-M, n+1+L, n+1\}$ are positive for certain $n \in \{1, \ldots, M-1\}$. As the additional zeroes at $\breve{u}_\mu$ are removed, we can deform and simplify the integration contour C to the four straight lines (green), which pairwise enclose the CP zeroes (yellow), or equivalently, the four points (2.18) (black dots). Due to the double periodic complex plane, the integration paths at $\Re(u) = \pm K$ add up to zero. Note that in the ordered phase below T_c the smallest real zero u_1 reaches $\pm K$ and becomes complex, such that the integration contour has to be modified as indicated. In figure 4 the complex torus is depicted.

Summarizing the last steps, we have found an extremely compact representation for the partition function of the anisotropic square lattice Ising model on the rectangle as the determinant of a Hankel matrix $\mathbf{H} = \left[h_{i+j+1}\right]_{i,j=0}^{M/2-1}$,

$$Z = Z_1 \, \det \, \mathbf{H}, \qquad h_n = \frac{1}{2\pi \mathrm{i}} \oint_C \frac{1 - \mathrm{e}^{L\gamma-\theta}}{1 - \mathrm{e}^{\mathrm{i}(M\varphi-\omega)}} \, \chi^n \, \frac{\partial \gamma}{\partial u} \, \mathrm{d}u, \tag{3.28}$$

[11] n-fold poles (zeroes) have pole order n ($-n$).

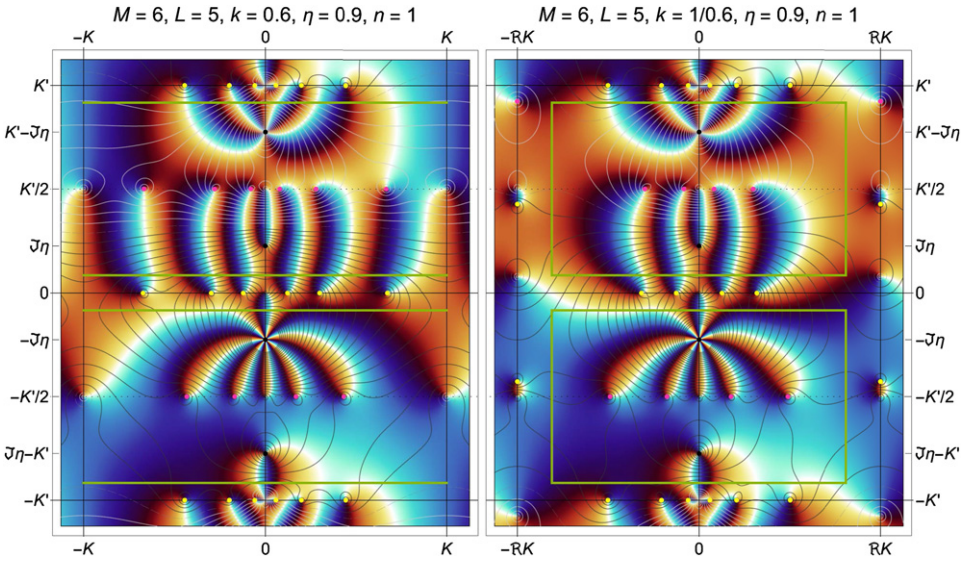

Figure 3. Complex structure of the integrand (3.27) for $M = 6$, $L = 5$, $n = 1$ and anisotropy $\eta = 0.9\eta_{\mathrm{iso}}$, above ($k = 0.6$, left) and below ($k^{-1} = 0.6$, right) the critical point. Yellow: M zeroes of the denominator, i.e., eigenvalues λ_μ of $\mathbf{T}$, and their para-conjugate. Pink: L zeroes of the numerator and their para-conjugate. Black: multiple zeroes/poles from (2.18a), with pole order $\{-4, 1, 7, 2\}$ from top to bottom in this case. Green: possible integration paths. The contour lines are at constant modulus, with a dashed gray line at 1, and light (dark) gray lines at powers of 2 below (above) 1. The complex phase is color coded, being {white, red, black, blue} at $\{1, \mathrm{i}, -1, -\mathrm{i}\}$, such that white turns to red (blue) at zeroes (poles) under ccw. rotation. Note that K becomes complex for $k > 1$.

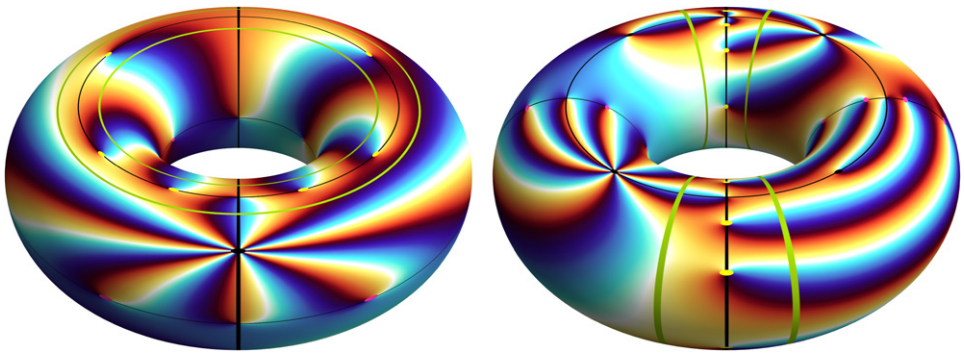

Figure 4. Complex structure of the integrand (3.27) from figure 3 (left), mapped onto a torus. These pictures might (or might not) be helpful to better understand the setup. Left: the upper circle is the real axis, with the odd zeroes of the denominator (yellow), the outer circle has $\Im(u) = -K'/2$, with the even zeroes of the numerator (pink), and the black point in front is at $-\eta$. The remaining zeroes are inside and at the bottom. Right: the top circle is the imaginary axis $\Re(u) = 0$, the front ring is the real axis. This representation corresponds to the original directions of the Ising model: the $\updownarrow$ direction goes along the $2M$ denominator zeroes (yellow) from front to back, the $\leftrightarrow$ direction goes along the $2L$ numerator zeroes (pink) from left to right, see also table 1.

with constant Z_1 from (3.23a). The h_n are Fourier coefficients (in the χ base) of a so-called symbol function with Fisher–Hartwig type singularities [90, 91] (see below), which is given by the ratio of two CPs. These polynomials are associated with the two directions as well as the corresponding BCs. As the considered system is invariant under an exchange of the two directions, the two CPs are directly related by the symmetry (1.5) of the underlying square lattice Ising model.

Note that the L zeroes v_ℓ of the numerator $1-\mathrm{e}^{L\gamma-\theta}$ correspond to the L eigenvalues of a hypothetical $L\times L$ transfer matrix $\tilde{\mathbf{T}}$ propagating in vertical direction, which would have been used in an alternative rotated setup. Only in the isotropic square system, where $L=M$ and $\mathcal{K}^{\leftrightarrow}=\mathcal{K}^{\updownarrow}$, these zeroes coincide with the swap-transformed zeroes, $v_\ell=\mathcal{S}(u_\mu)=\tilde{u}_\mu$. Unfortunately, we were not able to simplify the integral (3.28) in this symmetric case.

3.5. From Hankel to Toeplitz

The Hankel matrix (3.27) can be further transformed using the identities derived by Basor and Ehrhardt [92]. Using theorem 2.3, the symbols a and b, as well as the notation $T_M(a)$, $H_M(a)$ and $H_M[b]$ from [92], the determinant of $\mathbf{H}$, with elements (3.27), corresponds to the Hankel moment determinant $\det H_M[b]$ and can be transformed to the symmetric Toeplitz plus Hankel determinant $\det(T_M(a)+H_M(a))$, with the symbol

$$a(\zeta)=\mathrm{e}^{-\psi}\,b(\zeta_+)=\frac{1-\mathrm{e}^{L\gamma-\theta}}{1-\mathrm{e}^{\mathrm{i}(M\varphi-\omega)}}\,\frac{\partial\gamma}{\mathrm{i}\partial\varphi}, \tag{3.29}$$

and with the Fourier components [92, equation (3)]

$$a_n=a_{-n}=\frac{1}{2\pi}\oint_C a(\mathrm{e}^{\mathrm{i}\varphi})\,\mathrm{e}^{-\mathrm{i}n\varphi}\,\frac{\partial\varphi}{\partial u}\,\mathrm{d}u \tag{3.30a}$$

$$=\frac{1}{2\pi\mathrm{i}}\oint_C\frac{1-\mathrm{e}^{L\gamma-\theta}}{1-\mathrm{e}^{\mathrm{i}(M\varphi-\omega)}}\zeta^{-n}\,\frac{\partial\gamma}{\partial u}\,\mathrm{d}u. \tag{3.30b}$$

Note that (3.29) transforms to its reciprocal, $\mathcal{S}[a(\zeta)]=1/a(\zeta)$, under exchange of the two directions. The advantage of this representation is the occurrence of the simpler Fourier base ζ^{-n}, which eliminates the poles in the integrand stemming from $\zeta\to\infty$ at the points $u_{\infty,\infty}=\eta$ and $u_{0,\infty}=\mathrm{i}K'-\eta$, provided $L<M$ (as $n\geqslant 0$). We can therefore simplify the integration contour to a curve around the two remaining poles at $u_{\infty,0}=-\eta$ and $u_{0,0}=-\mathrm{i}K'+\eta$. However, for arbitrary L and M the pole order of the integrand (3.30b) at the four points (2.18) is $\{-n+2-M,-n+L-M,n+L,n\}$ and can be positive in all four cases, such that all four points must be enclosed by the contour.

Finally, from chapter 3 of [92] we borrow a clever transformation from the symmetric Toeplitz plus Hankel representation to a skew-symmetric $M\times M$ Toeplitz matrix $\hat{\mathbf{T}}$, with the result

$$\hat{\mathbf{T}}=\left[\sum_{\mu=1}^{M}\frac{2\mathrm{i}t^*\,\mathrm{e}^{L\gamma_\mu-\theta_\mu}}{P'_\chi(\chi_\mu)\sin\varphi_\mu}\cot\left(\frac{1}{2}\varphi_\mu\right)\sin\big[(i-j)\varphi_\mu\big]\right]_{i,j=0}^{M-1} \tag{3.31a}$$

$$=\left[\frac{1}{\pi\mathrm{i}}\oint_C\frac{1-\mathrm{e}^{L\gamma-\theta}}{1-\mathrm{e}^{\mathrm{i}(M\varphi-\omega)}}\cot\left(\frac{1}{2}\varphi\right)\sin[(i-j)\varphi]\,\frac{\partial\gamma}{\partial u}\,\mathrm{d}u\right]_{i,j=0}^{M-1}, \tag{3.31b}$$

such that the Pfaffian of $\hat{\mathbf{T}}$ fulfills $\mathrm{Pf}\,\hat{\mathbf{T}}=\det\mathbf{H}$, and therefore

$$Z=Z_1\,\mathrm{Pf}\,\hat{\mathbf{T}}. \tag{3.31c}$$

As before, the integration contour C can be freely deformed as long as it enclosed all zeroes u_μ or, alternatively, the four points (2.18).

4. Discussion

In this work, we showed that the partition function of the anisotropic square lattice Ising model on the $L \times M$ rectangle with open BCs in both directions is given by the determinant of an $M/2 \times M/2$ Hankel matrix $\mathbf{H}$, which equivalently can be written as the Pfaffian of a skew-symmetric $M \times M$ Toeplitz matrix $\hat{\mathbf{T}}$. The $M-1$ independent matrix elements of $\mathbf{H}$ or $\hat{\mathbf{T}}$ are Fourier coefficients of a symbol function (3.29), which is given by the ratio of two CPs. These polynomials are associated to the two directions $(\leftrightarrow, \updownarrow)$ of the system, encode the respective BCs, and are directly related through the symmetry of the square lattice Ising model under exchange of the two directions.

In the framework of the square lattice Ising model, Toeplitz matrices and determinants are well known in the context of bulk spatial correlation functions $\langle\sigma_{0,0}\sigma_{\ell,m}\rangle$ [4, 90, 93], eventually leading to the spontaneous magnetization for $\ell^2 + m^2 \to \infty$. Surprisingly, they now also appear in the exact expressions for the partition function Z of finite systems.

The considered anisotropic Ising model with open BCs in both directions is invariant under exchange of the two directions $\leftrightarrow$ and $\updownarrow$, such that both the system dimensions and the coupling constants are exchanged according to $L \overset{\mathcal{S}}{\longleftrightarrow} M$ and $\mathcal{K}^{\leftrightarrow} \overset{\mathcal{S}}{\longleftrightarrow} \mathcal{K}^{\updownarrow}$, see table 1. This *swap transformation* $\mathcal{S}$ (1.5) leads to the mapping of z and t to their respective duals, $(z,t) \overset{\mathcal{S}}{\mapsto} (t^*, z^*)$, as well as to the exchange of the eigenvalues and angles according to $\lambda \overset{\mathcal{S}}{\longleftrightarrow} \zeta$, $\gamma \overset{\mathcal{S}}{\longleftrightarrow} \mathrm{i}\varphi$ and $\theta \overset{\mathcal{S}}{\longleftrightarrow} \mathrm{i}\omega$. In the complex u-plane, it corresponds to a point reflection $(u,\eta) \overset{\mathcal{S}}{\mapsto} (\tilde{u},\tilde{\eta})$ of the complex torus at the point $\eta_{\mathrm{iso}} = \frac{1}{4}\mathrm{i}K'$ from (2.15). The elliptic modulus k, however, is invariant under this transformation. This symmetry must not be confused with the related duality transformation $\mathcal{D} : (z, t^*) \mapsto \mathcal{D}[(z, t^*)] = (t, z^*)$ of the bulk system, which maps a low-temperature system with spins $\sigma_{\ell,m}$ at $k > 1$ to a high-temperature system with the plaquette spins $\tilde{\sigma}_{\ell,m}$ at $k \mapsto \tilde{k} = k^{-1} < 1$, see figure 1. Note that in systems with boundaries, this transform is known to change the BCs, e.g., from open to fixed.

Table 1. Overview over the quantities used in this work. The transformation $\mathcal{S}$ (1.5) maps between the two directions of the model. The right columns show the relation of our notation to the work of Baxter [7], where the transfer matrix propagated vertically.

Direction	$\leftrightarrow$	$\updownarrow$	$\updownarrow$ [7]	$\leftrightarrow$ [7]
Number of sites	L	M	M	N
Reduced coupling	$\mathcal{K}^{\leftrightarrow}$	$\mathcal{K}^{\updownarrow}$	H	H'
Weights	(z,t)	(t^*,z^*)	(t^*,u^*)	(u,t)
Transfer matrix	$\boldsymbol{\mathcal{T}}$	$\mathbf{Q}$	$\hat{V}_2\hat{V}_1$	—
Eigenvalues	λ	ζ	λ	z
Angles	γ	$\mathrm{i}\varphi$	—	—
Boundary angles	θ	$\mathrm{i}\omega$	—	—
Characteristic polynomial	$1-\mathrm{e}^{L\gamma-\theta}$	$1-\mathrm{e}^{\mathrm{i}(M\varphi-\omega)}$	—	[7, (3.21)]
Elliptic variables	(u,η)	$(\tilde{u},\tilde{\eta})$	$(r,\nu/2)$	$(\bar{r},\bar{\nu}/2)$
Elliptic modulus		k		k^{-1}
$\Im$(CP zeroes)	$(0,K')$	$\pm K'/2$	—	—

During the present calculation, it was tried to find a representation of the partition function Z that is formally symmetric under the exchange of the two directions, mediated by the transformation $\mathcal{S}$. While the symbol function $a(\zeta)$ from (3.29) already fulfills $\mathcal{S}[a(\zeta)] = 1/a(\zeta)$, the transformation $\mathcal{S}$ exchanges the system dimensions $L \overset{\mathcal{S}}{\longleftrightarrow} M$ and therefore changes the dimensions of the involved matrices, such that, e.g., a representation using $(M+L)\times(M+L)$ dimensional matrices might be necessary for a unified description.

The obtained results might possibly be rewritten using elliptic product identities, as done by Baxter [7] in the thermodynamic limit. The ultimate goal would be to use elliptic determinant evaluations as done successfully by Iorgov and Lisovyy [84], which might lead to a closed product representation of the partition function.

We expect that our results can be extended to other BCs by using the corresponding CPs, these generalizations are left for future work.

From the Toeplitz determinant representation of the partition function, it is rather straightforward to derive the (anisotropic) scaling limit $L, M \to \infty$, $T \to T_\mathrm{c}$ at fixed scaling variables $x_\updownarrow \equiv (T/T_\mathrm{c} - 1)(M/\xi_0^\updownarrow)^{1/\nu}$ and $\rho \equiv (L/\xi_0^\leftrightarrow)/(M/\xi_0^\updownarrow)$ using Szegő's theorem [93–95]. This task will be addressed in a forthcoming work.

Acknowledgments

The author is grateful to Hendrik Oppenberg, Felix M Schmidt and Wolfhard Janke for helpful discussions and inspirations. Discussions with Jan Büddefeld, Luca Cervellera and Nils Gluth are acknowledged. This work was partially supported by the Deutsche Forschungsgemeinschaft through Grant HU 2303/1-1.

Data availability statement

No new data were created or analysed in this study.

Appendix A. Useful elliptic identities

In this appendix we will list identities arising from the elliptic parametrization. We also simplify expressions given in chapter 6 of [9]. Following McCoy and Wu [16] (who used $\alpha_1^{\pm1}, \alpha_2^{\pm1}$) and Iorgov and Lisovyy [84] (who used $\alpha^{\pm1}, \beta^{\pm1}$), we introduce abbreviations for products and ratios of z and t, however we again utilize Glashier's notation (2.6) and define the constants

$$\lambda_\mathrm{n} \equiv tz, \qquad \lambda_\mathrm{s} \equiv \frac{1}{tz}, \qquad \lambda_\mathrm{c} \equiv \frac{t}{z}, \qquad \lambda_\mathrm{d} \equiv \frac{z}{t}, \tag{A.1}$$

with $\lambda_\mathrm{n}\lambda_\mathrm{s} = \lambda_\mathrm{c}\lambda_\mathrm{d} = 1$. This leads to the identities

$$\mathrm{sn}^2\,\eta = -\lambda_\mathrm{n}k^{-1}, \quad \mathrm{cn}^2\,\eta = \frac{\lambda_\mathrm{n}\lambda_{\mathrm{n},-}}{tt_-} = 1 + \lambda_\mathrm{n}k^{-1}, \quad \mathrm{dn}^2\,\eta = \frac{\lambda_\mathrm{n}\lambda_{\mathrm{n},-}}{zz_-} = 1 + \lambda_\mathrm{n}k. \tag{A.2}$$

Furthermore, We list relations to the primary reduced couplings $\mathcal{K}^\delta$ from (1.1),

$$t = \exp(-2\mathcal{K}^\updownarrow), \qquad t_+ = \cosh(2\mathcal{K}^\updownarrow), \qquad t_- = -\sinh(2\mathcal{K}^\updownarrow), \tag{A.3a}$$

$$z = \tanh\,\mathcal{K}^\leftrightarrow, \qquad z_+ = \coth(2\mathcal{K}^\leftrightarrow), \qquad z_- = -\mathrm{csch}(2\mathcal{K}^\leftrightarrow), \tag{A.3b}$$

whereas for the dual couplings z^*, t^* the directions $\leftrightarrow$ and $\updownarrow$ are to be exchanged,

$$z^* = \exp(-2\mathcal{K}^{\leftrightarrow}), \quad z^*_+ = \cosh(2\mathcal{K}^{\leftrightarrow}), \quad z^*_- = -\sinh(2\mathcal{K}^{\leftrightarrow}), \tag{A.3c}$$

$$t^* = \tanh\,\mathcal{K}^{\updownarrow}, \qquad t^*_+ = \coth(2\mathcal{K}^{\updownarrow}), \qquad t^*_- = -\operatorname{csch}(2\mathcal{K}^{\updownarrow}). \tag{A.3d}$$

Defining the dual primary reduced couplings $\tilde{\mathcal{K}}^\delta$ via

$$\exp(-2\tilde{\mathcal{K}}^\delta) = \tanh\,\mathcal{K}^\delta, \tag{A.4}$$

we conclude from (2.12) that the following simple relations hold between $\tilde{\mathcal{K}}^\delta$ and η,

$$2\mathrm{i}\tilde{\mathcal{K}}^{\updownarrow} = \mathrm{am}(2\eta), \qquad 2\mathrm{i}\tilde{\mathcal{K}}^{\leftrightarrow} = \mathrm{am}(2\tilde{\eta}), \tag{A.5}$$

such that the Jacobi amplitude (2.1) represents a direct connection between the physical reduced couplings $\mathcal{K}^\delta$ and the parameter η, and (2.14) can be written using the elliptic integral of the first kind, cf (2.2),

$$2\eta = F(2\mathrm{i}\tilde{\mathcal{K}}^{\updownarrow}, k) = \mathrm{i}K' - F(2\mathrm{i}\tilde{\mathcal{K}}^{\leftrightarrow}, k). \tag{A.6}$$

We now turn to the eigenvalues λ and ζ. Defining the abbreviation

$$Q(u,\eta) \equiv \sqrt{\lambda_\mathrm{n} - \lambda} = \sqrt{\frac{(k\,\mathrm{sn}^2\,\eta)^2 - 1}{k\,\mathrm{sn}^2\,u - k\,\mathrm{sn}^2\,\eta}}, \tag{A.7}$$

we can express the four roots from chapter 6 of [9] as meromorphic functions of u, eliminating the ambiguous signs of the square roots,

$$\sqrt{\lambda_\mathrm{n} - \lambda} = Q(u,\eta)\frac{\mathrm{nn}\,u}{\mathrm{nn}\,\eta}, \qquad \sqrt{\lambda_\mathrm{s} - \lambda} = Q(u,\eta)\frac{\mathrm{sn}\,u}{\mathrm{sn}\,\eta}, \tag{A.8a}$$

$$\sqrt{\lambda_\mathrm{c} - \lambda} = Q(u,\eta)\frac{\mathrm{cn}\,u}{\mathrm{cn}\,\eta}, \qquad \sqrt{\lambda_\mathrm{d} - \lambda} = Q(u,\eta)\frac{\mathrm{dn}\,u}{\mathrm{dn}\,\eta}. \tag{A.8b}$$

Note that we have used the trivial elliptic function $\mathrm{nn}\,u \equiv 1$ in order to illustrate the systematics. Using (2.13) we can derive analog expressions for ζ,

$$\sqrt{\zeta_\mathrm{n} - \zeta} = Q(\tilde{u},\tilde{\eta})\frac{\mathrm{nn}\,\tilde{u}}{\mathrm{nn}\,\tilde{\eta}}, \qquad \sqrt{\zeta_\mathrm{s} - \zeta} = Q(\tilde{u},\tilde{\eta})\frac{\mathrm{sn}\,\tilde{u}}{\mathrm{sn}\,\tilde{\eta}}, \tag{A.9a}$$

$$\sqrt{\zeta_\mathrm{c} - \zeta} = Q(\tilde{u},\tilde{\eta})\frac{\mathrm{cn}\,\tilde{u}}{\mathrm{cn}\,\tilde{\eta}}, \qquad \sqrt{\zeta_\mathrm{d} - \zeta} = Q(\tilde{u},\tilde{\eta})\frac{\mathrm{dn}\,\tilde{u}}{\mathrm{dn}\,\tilde{\eta}}, \tag{A.9b}$$

where we defined

$$\zeta_\mathrm{n} \equiv z^* t^*, \qquad \zeta_\mathrm{s} \equiv \frac{1}{z^* t^*}, \qquad \zeta_\mathrm{c} \equiv \frac{z^*}{t^*}, \qquad \zeta_\mathrm{d} \equiv \frac{t^*}{z^*}, \tag{A.10}$$

in analogy to (A.1). From (A.8a) and (A.9a) we further derive

$$\lambda = \frac{1 - k^2\,\mathrm{sn}^2\,u\,\mathrm{sn}^2\,\eta}{k(\mathrm{sn}^2\,u - \mathrm{sn}^2\,\eta)}, \qquad \zeta = \frac{1 - k^2\,\mathrm{sn}^2\,\tilde{u}\,\mathrm{sn}^2\tilde{\eta}}{k(\mathrm{sn}^2\,\tilde{u} - \mathrm{sn}^2\,\tilde{\eta})}, \tag{A.11a}$$

which can be expressed using (1.2),

$$\lambda^* = -\frac{(k\,\mathrm{sn}^2\,u)^*}{(k\,\mathrm{sn}^2\,\eta)^*}, \qquad \zeta^* = -\frac{(k\,\mathrm{sn}^2\,\tilde{u})^*}{(k\,\mathrm{sn}^2\,\tilde{\eta})^*}. \tag{A.11b}$$

Inserting the elliptic expressions (A.8) into (I.46) we find

$$\sin\frac{\varphi}{2} = -\frac{\sqrt{\lambda_\mathrm{c}-\lambda}\sqrt{\lambda_\mathrm{d}-\lambda}}{2\sqrt{\lambda t_- z_-}} = -\frac{Q^2(u,\eta)}{2\sqrt{\lambda t_- z_-}}\frac{\mathrm{cn}\,u}{\mathrm{cn}\,\eta}\frac{\mathrm{dn}\,u}{\mathrm{dn}\,\eta}, \tag{A.12a}$$

$$\cos\frac{\varphi}{2} = \frac{\sqrt{\lambda_\mathrm{n}-\lambda}\sqrt{\lambda_\mathrm{s}-\lambda}}{2\mathrm{i}\sqrt{\lambda t_- z_-}} = \frac{Q^2(u,\eta)}{2\mathrm{i}\sqrt{\lambda t_- z_-}}\frac{\mathrm{nn}\,u}{\mathrm{nn}\,\eta}\frac{\mathrm{sn}\,u}{\mathrm{sn}\,\eta}, \tag{A.12b}$$

$$\tan\frac{\varphi}{2} = \frac{1}{\mathrm{i}}\frac{\sqrt{\lambda_\mathrm{c}-\lambda}\sqrt{\lambda_\mathrm{d}-\lambda}}{\sqrt{\lambda_\mathrm{n}-\lambda}\sqrt{\lambda_\mathrm{s}-\lambda}} = \frac{1}{\mathrm{i}}\frac{\mathrm{nn}\,\eta}{\mathrm{nn}\,u}\frac{\mathrm{sn}\,\eta}{\mathrm{sn}\,u}\frac{\mathrm{cn}\,u}{\mathrm{cn}\eta}\frac{\mathrm{dn}\,u}{\mathrm{dn}\,\eta}, \tag{A.12c}$$

while (I.47) at the eigenvalues λ_μ become

$$\pm\sin\frac{M\varphi_\mu}{2} = \sqrt{t}\frac{\sqrt{\lambda_\mathrm{s}-\lambda_\mu}\sqrt{\lambda_\mathrm{d}-\lambda_\mu}}{2\sqrt{\lambda_\mu t_- \lambda_{\mu,-}}} = \frac{\sqrt{t}}{2}\frac{Q^2(u_\mu,\eta)}{\sqrt{\lambda_\mu t_- \lambda_{\mu,-}}}\frac{\mathrm{sn}\,u_\mu}{\mathrm{sn}\,\eta}\frac{\mathrm{dn}\,u_\mu}{\mathrm{dn}\,\eta}, \tag{A.13a}$$

$$\pm\cos\frac{M\varphi_\mu}{2} = \frac{1}{\sqrt{t}}\frac{\sqrt{\lambda_\mathrm{n}-\lambda_\mu}\sqrt{\lambda_\mathrm{c}-\lambda_\mu}}{2\mathrm{i}\sqrt{\lambda_\mu t_- \lambda_{\mu,-}}} = \frac{1}{2\mathrm{i}\sqrt{t}}\frac{Q^2(u_\mu,\eta)}{\sqrt{\lambda_\mu t_- \lambda_{\mu,-}}}\frac{\mathrm{nn}\,u_\mu}{\mathrm{nn}\,\eta}\frac{\mathrm{cn}\,u_\mu}{\mathrm{cn}\,\eta}, \tag{A.13b}$$

$$\tan\frac{M\varphi_\mu}{2} = \mathrm{i}t\frac{\sqrt{\lambda_\mathrm{s}-\lambda_\mu}\sqrt{\lambda_\mathrm{d}-\lambda_\mu}}{\sqrt{\lambda_\mathrm{n}-\lambda_\mu}\sqrt{\lambda_\mathrm{c}-\lambda_\mu}} = \frac{\mathrm{sn}\,u_\mu\,\mathrm{dn}\,u_\mu}{\mathrm{nn}\,u_\mu\,\mathrm{cn}\,u_\mu}. \tag{A.13c}$$

We additionally list the identities

$$t_- z_- \mathrm{i}\,\sin\varphi = -\frac{1}{2\lambda}\sqrt{\lambda_\mathrm{n}-\lambda}\sqrt{\lambda_\mathrm{s}-\lambda}\sqrt{\lambda_\mathrm{c}-\lambda}\sqrt{\lambda_\mathrm{d}-\lambda} \tag{A.14a}$$

$$= \sqrt{\lambda_{\mathrm{s},+}-\lambda_+}\sqrt{\lambda_{\mathrm{d},+}-\lambda_+} \tag{A.14b}$$

$$= -\frac{Q^4(u,\eta)}{2\lambda}\frac{\mathrm{nn}\,u}{\mathrm{nn}\,\eta}\frac{\mathrm{sn}\,u}{\mathrm{sn}\,\eta}\frac{\mathrm{cn}\,u}{\mathrm{cn}\,\eta}\frac{\mathrm{dn}\,u}{\mathrm{dn}\,\eta}, \tag{A.14c}$$

as well as

$$\sqrt{2t_- z_-}\,\mathrm{i}\,\sin\frac{\varphi}{2} = \sqrt{\lambda_{\mathrm{d},+}-\lambda_+}, \quad \sqrt{2t_- z_-}\,\cos\frac{\varphi}{2} = \sqrt{\lambda_{\mathrm{s},+}-\lambda_+}. \tag{A.14d}$$

Using the addition theorem [81, (2.4.22)]

$$k\,\mathrm{sn}\,u\,\mathrm{sn}\,v = k\frac{\mathrm{cn}(u-v)-\mathrm{cn}(u+v)}{\mathrm{dn}(u-v)+\mathrm{dn}(u+v)} = \frac{1}{k}\frac{\mathrm{dn}(u-v)-\mathrm{dn}(u+v)}{\mathrm{cn}(u-v)+\mathrm{cn}(u+v)} \tag{A.15}$$

we derive the important identities

$$\lambda = \mathrm{e}^\gamma = -k\frac{\mathrm{cn}(2u)+\mathrm{cn}(2\eta)}{\mathrm{dn}(2u)-\mathrm{dn}(2\eta)} = -\frac{1}{k}\frac{\mathrm{dn}(2u)+\mathrm{dn}(2\eta)}{\mathrm{cn}(2u)-\mathrm{cn}(2\eta)}, \tag{A.16a}$$

$$\lambda_+ = \cosh\gamma = -k\frac{\mathrm{cn}(2u)\mathrm{dn}(2u)+\mathrm{cn}(2\eta)\mathrm{dn}(2\eta)}{\mathrm{dn}^2(2u)-\mathrm{dn}^2(2\eta)}, \tag{A.16b}$$

$$\lambda_- = \sinh\gamma = -k\frac{\mathrm{cn}(2u)\mathrm{dn}(2\eta)+\mathrm{cn}(2\eta)\mathrm{dn}(2u)}{\mathrm{dn}^2(2u)-\mathrm{dn}^2(2\eta)}, \tag{A.16c}$$

and, by the swap transformation (2.13),

$$\zeta = \mathrm{e}^{\mathrm{i}\varphi} = -\frac{\mathrm{ds}(2u) + \mathrm{ds}(2\eta)}{\mathrm{cs}(2u) - \mathrm{cs}(2\eta)} = -\frac{\mathrm{cs}(2u) + \mathrm{cs}(2\eta)}{\mathrm{ds}(2u) - \mathrm{ds}(2\eta)}, \tag{A.17a}$$

$$\zeta_+ = \cos\,\varphi = -\frac{\mathrm{ds}(2u)\mathrm{cs}(2u) + \mathrm{ds}(2\eta)\mathrm{cs}(2\eta)}{\mathrm{cs}^2(2u) - \mathrm{cs}^2(2\eta)}, \tag{A.17b}$$

$$\zeta_- = \mathrm{i}\,\sin\,\varphi = -\frac{\mathrm{ds}(2u)\mathrm{cs}(2\eta) + \mathrm{ds}(2\eta)\mathrm{cs}(2u)}{\mathrm{cs}^2(2u) - \mathrm{cs}^2(2\eta)}, \tag{A.17c}$$

which express the eigenvalues λ and ζ as functions of $2u$.

We now turn to derivatives. From (2.16) and

$$\frac{\partial}{\partial u}\,\log\,\mathrm{sn}(u \pm \eta) = \frac{\mathrm{cn}(u \pm \eta)\mathrm{dn}(u \pm \eta)}{\mathrm{sn}(u \pm \eta)} = k\lambda_-[\mathrm{sn}(2u) \mp \mathrm{sn}(2\eta)] \tag{A.18}$$

we see that the derivatives of φ and γ w.r.t. u become

$$\frac{1}{2}\frac{\partial\varphi}{\partial u} = \mathrm{i}k\,\mathrm{sn}(2\eta)\,\lambda_- = \frac{1}{z_-}\,\sinh\,\gamma = -\frac{\sin\,\varphi}{\sin\,\omega}, \tag{A.19a}$$

$$\frac{1}{2}\frac{\partial\gamma}{\partial u} = -k\,\mathrm{sn}(2u)\,\lambda_- = t_-\,\sin\,\varphi = \mathrm{i}\,\frac{\sinh\,\gamma}{\sinh\,\theta}, \tag{A.19b}$$

from which other identities, such as

$$\frac{\partial\gamma}{\partial\varphi} = -t_-\,\sin\,\omega = t_-z_-\frac{\sin\,\varphi}{\sinh\,\gamma}, \qquad \frac{\partial\chi}{\partial u} = \frac{\chi^2 - 4}{\sin\,\omega}, \tag{A.20}$$

are easily calculated.

In the ordered phase where $k > 1$, the angle φ_1 becomes complex [9, chapter 6], leading to a complex value of u_1. The correct mapping from the eigenvalues λ_μ to the elliptic variable u_μ, respecting this behavior and being valid at arbitrary temperatures, can be expressed using the inverse Jacobi dn, see (A.8),

$$u_\mu = \mathrm{dn}^{(-1)}\left[\mathrm{dn}\,\eta\,\frac{\sqrt{\lambda_\mathrm{d} - \lambda_\mu}}{\sqrt{\lambda_\mathrm{n} - \lambda_\mu}}\right]. \tag{A.21}$$

While it is tempting to utilize the simpler relation (2.19)

$$u_\mu = \frac{1}{2}F(M\varphi_\mu, k), \tag{A.22}$$

it will not give correct results for even μ and below T_c, because the elliptic integral F does not have the correct branch cut positions for these cases.

Appendix B. A block Hankel matrix identity

Let $\mathcal{V}_{g,x}$ be the generalized $1 \times B$ block Vandermonde matrix with $M \times N$ blocks

$$\mathcal{V}_{g,x} \equiv \left[g_\mu^b\,x_\mu^n\right]_{b=0;\ \mu=1,\ n=0}^{B-1\quad M\quad N-1} = \left[\mathbf{G}^b\,\mathbf{V}_x\right]_{b=0}^{B-1}, \tag{B.1}$$

with

$$\mathbf{V}_{\boldsymbol{x}} \equiv \left[x_\mu^n\right]_{\mu=1,\,n=0}^{M\quad N-1}, \qquad \mathbf{G} \equiv \left[\delta_{\mu\nu}\, g_\mu\right]_{\mu,\nu=1}^{M}. \tag{B.2}$$

As an example, for $M = 4$, $B = 3$ and $N = 3$ we have

$$\boldsymbol{\mathcal{V}}_{\boldsymbol{g},\boldsymbol{x}} = \left[\begin{array}{ccc|ccc|ccc} 1 & x_1 & x_1^2 & g_1 & g_1x_1 & g_1x_1^2 & g_1^2 & g_1^2x_1 & g_1^2x_1^2 \\ 1 & x_2 & x_2^2 & g_2 & g_2x_2 & g_2x_2^2 & g_2^2 & g_2^2x_2 & g_2^2x_2^2 \\ 1 & x_3 & x_3^2 & g_3 & g_3x_3 & g_3x_3^2 & g_3^2 & g_3^2x_3 & g_3^2x_3^2 \\ 1 & x_4 & x_4^2 & g_4 & g_4x_4 & g_4x_4^2 & g_4^2 & g_4^2x_4 & g_4^2x_4^2 \end{array}\right]. \tag{B.3}$$

Furthermore, let $\mathbf{D}$ be an arbitrary $M \times M$ diagonal matrix. Then, the $B \times B$ block Hankel matrix with $N \times N$ blocks

$$\boldsymbol{\mathcal{H}}_{\boldsymbol{g},\boldsymbol{x}} \equiv \left[\sum_{\mu=1}^{M} \mathrm{d}_\mu g_\mu^{a+b}\, x_\mu^{m+n}\right]_{a,b=0;\,m,n=0}^{B-1\quad N-1} = \left[\mathbf{V}_{\boldsymbol{x}}^\top\, \mathbf{D}\, \mathbf{G}^{a+b}\, \mathbf{V}_{\boldsymbol{x}}\right]_{a,b=0}^{B-1} \tag{B.4}$$

trivially fulfills the identity

$$\boldsymbol{\mathcal{H}}_{\boldsymbol{g},\boldsymbol{x}} = \boldsymbol{\mathcal{V}}_{\boldsymbol{g},\boldsymbol{x}}^\top \mathbf{D} \boldsymbol{\mathcal{V}}_{\boldsymbol{g},\boldsymbol{x}}. \tag{B.5}$$

Note that the upper left block $(\boldsymbol{\mathcal{H}}_{\boldsymbol{g},\boldsymbol{x}})_{0,0} = \mathbf{V}_{\boldsymbol{x}}^\top\, \mathbf{D}\, \mathbf{V}_{\boldsymbol{x}}$ is free of g_μ and is therefore a usual Vandermonde product in x_μ. Consequently, if the matrix $\mathbf{D}$ is set to the diagonal matrix $\mathbf{D}_{\boldsymbol{x}}$ with the reciprocal first derivatives of the CP $P_{\boldsymbol{x}}(x)$ from (3.17),

$$\mathbf{D}_{\boldsymbol{x}} \equiv \left[\frac{\delta_{\mu\nu}}{P'_{\boldsymbol{x}}(x_\mu)}\right]_{\mu,\nu=1}^{M}, \tag{B.6}$$

and if additionally $M \geqslant 2N$, then $(\mathbf{H}_{\boldsymbol{g},\boldsymbol{x}})_{0,0}$ vanishes identically. For $B = 2$ and $N = M/2$, this leads to equation (3.20).

Appendix C. More characteristic polynomials

In [11] we used the finite-size scaling limit of $P_{\boldsymbol{\lambda}_+}$ to locate the zeroes in the complex plane and to perform the corresponding Cauchy integrals. We had to distinguish between even and odd zeroes and defined an alternating counting polynomial from $P_{\boldsymbol{\lambda}_+}$. Now we will demonstrate that it is much easier to analyze the complex structure of the system by using the CP of the transfer matrix $\mathbf{T}$ instead of $\mathbf{T}_+$. While it is possible but cumbersome to derive the CP of $\mathbf{T}$, with eigenvalues λ_μ,

$$P_{\boldsymbol{\lambda}}(\lambda) \equiv \det(\lambda\mathbf{1} - \mathbf{T}) = \prod_{\mu=1}^{M} (\lambda - \lambda_\mu) \tag{C.1}$$

from scratch analogously to (1.19a), cf [9], we instead proceed in a much simpler way and derive it directly from (3.2): using (1.3), we first factorize the right-hand side of (1.19a),

$$P_{\boldsymbol{\lambda}_+}(\lambda_+) = \prod_{\mu=1}^{M} (\lambda_+ - \lambda_{\mu,+}) = \prod_{\mu=1}^{M} \frac{(\lambda - \lambda_\mu)(\lambda^{-1} - \lambda_\mu)}{2(0 - \lambda_\mu)} = \frac{1}{2^M t} P_{\boldsymbol{\lambda}}(\lambda) P_{\boldsymbol{\lambda}}(\lambda^{-1}), \tag{C.2}$$

as $\lambda_{\mu,+} = \lambda_{+,\mu}$ and, cf (I.35),

$$P_{\boldsymbol{\lambda}}(0) = \det(-\mathbf{T}) = \det\,\mathbf{T} = t. \tag{C.3}$$

Employing the trigonometric factorization identity

$$\frac{\sin(M\varphi-\omega)}{\sin(-\omega)} = \frac{\sin\left(\frac{1}{2}[M\varphi-\omega]\right)}{\sin\left(-\frac{1}{2}\omega\right)}\frac{\cos\left(\frac{1}{2}[M\varphi-\omega]\right)}{\cos\left(-\frac{1}{2}\omega\right)} \tag{C.4}$$

as well as the identities

$$\begin{aligned}&\lambda(\check{u})\lambda(u) = 1, \quad \varphi(\check{u}) = -\varphi(u), \quad \omega(\check{u}) + \omega(u) = \pi,\\ &\cot\left[\frac{1}{2}\omega(\check{u})\right] = \tan\left[\frac{1}{2}\omega(u)\right],\end{aligned} \tag{C.5}$$

with inversion transform $u \mapsto \check{u} \equiv u + \mathrm{i}K'$, we see that $P_{\boldsymbol{\lambda}}(\lambda)$ and $P_{\boldsymbol{\lambda}}(\lambda^{-1})$ are given by the remarkably simple formulas

$$P_{\boldsymbol{\lambda}}(\lambda) = (1-t^*)(-t_-z_-\lambda)^{\frac{M}{2}}\left[\cos\left(\frac{1}{2}M\varphi\right) - \cot\left(\frac{1}{2}\omega\right)\sin\left(\frac{1}{2}M\varphi\right)\right] \tag{C.6a}$$

$$= (1-t^*)(-t_-z_-\lambda)^{\frac{M}{2}}\frac{\sin\left(\frac{1}{2}[M\varphi-\omega]\right)}{\sin\left(-\frac{1}{2}\omega\right)} \tag{C.6b}$$

$$= (1-t^*)\left(-\frac{t_-z_-\lambda}{\zeta}\right)^{\frac{M}{2}}\frac{1-\mathrm{e}^{\mathrm{i}(M\varphi-\omega)}}{1-\mathrm{e}^{-\mathrm{i}\omega}}, \tag{C.6c}$$

$$P_{\boldsymbol{\lambda}}(\lambda^{-1}) = (1-t^*)\left(-t_-z_-\lambda^{-1}\right)^{\frac{M}{2}}\left[\cos\left(\frac{1}{2}M\varphi\right) + \tan\left(\frac{1}{2}\omega\right)\sin\left(\frac{1}{2}M\varphi\right)\right] \tag{C.6d}$$

$$= (1-t^*)\left(-t_-z_-\lambda^{-1}\right)^{\frac{M}{2}}\frac{\cos\left(\frac{1}{2}[M\varphi-\omega]\right)}{\cos\left(-\frac{1}{2}\omega\right)} \tag{C.6e}$$

$$= (1-t^*)\left(-\frac{t_-z_-}{\lambda\zeta}\right)^{\frac{M}{2}}\frac{1+\mathrm{e}^{\mathrm{i}(M\varphi-\omega)}}{1+\mathrm{e}^{-\mathrm{i}\omega}}. \tag{C.6f}$$

The additional factor $(-\lambda)^{M/2}$ in $P_{\boldsymbol{\lambda}}(\lambda)$ follows from (C.3) in the known limits $\lambda \to \{0,\infty\}$, see (2.18). Utilizing a factorization similar to (C.2), the CP of $\mathbf{T}_-$ can also be derived,

$$\begin{aligned}P_{\boldsymbol{\lambda}_-}(\lambda_-) &= \prod_{\mu=1}^{M}(\lambda_- - \lambda_{\mu,-})\\ &= \prod_{\mu=1}^{M}\frac{(\lambda-\lambda_\mu)(-\lambda^{-1}-\lambda_\mu)}{2(0-\lambda_\mu)}\\ &= \frac{1}{2^M t}P_{\boldsymbol{\lambda}}(\lambda)P_{\boldsymbol{\lambda}}(-\lambda^{-1}).\end{aligned} \tag{C.7}$$

Finally, from (3.25) and Liouville's theorem [5, 15.3] we derived the CPs

$$P_\zeta(\zeta) = (1-t^*)\frac{1-\mathrm{e}^{\mathrm{i}(M\varphi-\omega)}}{1-\mathrm{e}^{-\mathrm{i}\omega}}\prod_{\mu=1}^{M}\frac{\mathrm{sn}(\eta+u_\mu)}{\mathrm{sn}(u+u_\mu)}, \tag{C.8}$$

$$P_\zeta(\zeta^{-1}) = (1-t^*)\frac{1+\mathrm{e}^{-\mathrm{i}(M\varphi-\omega)}}{1+\mathrm{e}^{\mathrm{i}\omega}}\prod_{\mu=1}^{M} k\,\mathrm{sn}(\eta+u_\mu)\mathrm{sn}(u+u_\mu). \tag{C.9}$$

Appendix D. Some product identities

Using the CPs (3.2), (C.6) and (C.7), we have the following identities (remember that M is even): the determinants are given by

$$\det\mathbf{T} = \prod_{\mu=1}^{M}\lambda_\mu = P_{\boldsymbol{\lambda}}(0) = t, \tag{D.1a}$$

$$\det\mathbf{T}_- = \prod_{\mu=1}^{M}\lambda_{\mu,-} = P_{\boldsymbol{\lambda}_-}(0) = (1-t^{*2})\left(\frac{\mathrm{i}z_-}{1-t^{*2}}\right)^M, \tag{D.1b}$$

$$\det\mathbf{T}_+ = \prod_{\mu=1}^{M}\lambda_{\mu,+} = P_{\boldsymbol{\lambda}_+}(0) = (1-t^{*2})\left(\frac{t_-z_-}{2}\right)^M\frac{\sin(M\varphi_{\lambda_+\to 0}-\omega_{\lambda_+\to 0})}{\sin(-\omega_{\lambda_+\to 0})}, \tag{D.1c}$$

with (2.18) and

$$u_{\lambda_+\to 0} = \mathrm{sn}^{(-1)}\sqrt{\frac{(\mathrm{i}\lambda_\mathrm{n})^*}{\mathrm{i}k}}, \qquad u_{\lambda_-\to 0} = K+\frac{1}{2}\mathrm{i}K'. \tag{D.2}$$

Furthermore, we have the following product identities for the Jacobi elliptic functions

$$\prod_{\mu=1}^{M}\sqrt{-tz}\,\frac{\mathrm{sn}\,u_\mu}{\mathrm{sn}\,\eta} = \sqrt{1-M\lambda_{\mathrm{s},-}z_-^{-1}}, \tag{D.3a}$$

$$\prod_{\mu=1}^{M}\sqrt{\mathrm{i}z}\,\frac{\mathrm{cn}\,u_\mu}{\mathrm{cn}\,\eta} = 1, \tag{D.3b}$$

$$\prod_{\mu=1}^{M}\sqrt{\mathrm{i}t}\,\frac{\mathrm{dn}\,u_\mu}{\mathrm{dn}\,\eta} = \sqrt{1+M\lambda_{\mathrm{d},-}z_-^{-1}}. \tag{D.3c}$$

For products over λ_μ we find the identities

$$\prod_{\mu=1}^{M}(\lambda_\mathrm{n}-\lambda_\mu) = P_{\boldsymbol{\lambda}}(\lambda_\mathrm{n}) = (1-t^*)(t_-z_-\lambda_\mathrm{n})^{\frac{M}{2}}, \tag{D.4a}$$

$$\prod_{\mu=1}^{M}(\lambda_\mathrm{c}-\lambda_\mu) = P_{\boldsymbol{\lambda}}(\lambda_\mathrm{c}) = (1-t^*)(-t_-z_-\lambda_\mathrm{c})^{\frac{M}{2}}, \tag{D.4b}$$

$$\prod_{\mu=1}^{M}(\lambda_{\rm s}-\lambda_\mu)=P_{\boldsymbol{\lambda}}(\lambda_{\rm s})=(1-t^*)(t_-z_-\lambda_{\rm s})^{\frac{M}{2}}\left(1-M\lambda_{{\rm s},-}z_-^{-1}\right), \tag{D.4c}$$

$$\prod_{\mu=1}^{M}(\lambda_{\rm d}-\lambda_\mu)=P_{\boldsymbol{\lambda}}(\lambda_{\rm d})=(1-t^*)(-t_-z_-\lambda_{\rm d})^{\frac{M}{2}}\left(1+M\lambda_{{\rm d},-}z_-^{-1}\right), \tag{D.4d}$$

and for products over ζ_μ we derive

$$\prod_{\mu=1}^{M}\sin\frac{\varphi_\mu}{2}=\frac{1-t^*}{(2{\rm i})^M\sqrt{t}}\sqrt{1+M\lambda_{{\rm d},-}z_-^{-1}}, \tag{D.5a}$$

$$\prod_{\mu=1}^{M}\cos\frac{\varphi_\mu}{2}=\frac{1-t^*}{2^M\sqrt{t}}\sqrt{1-M\lambda_{{\rm s},-}z_-^{-1}}, \tag{D.5b}$$

$$\prod_{\mu=1}^{M}\tan\frac{\varphi_\mu}{2}=(-1)^{M/2}\frac{\sqrt{1+M\lambda_{{\rm d},-}z_-^{-1}}}{\sqrt{1-M\lambda_{{\rm s},-}z_-^{-1}}}=\prod_{\mu=1}^{M}{\rm e}^{-\theta_\mu}=\prod_{\mu=1}^{M}{\rm e}^{-\psi_\mu}. \tag{D.5c}$$

Finally, from the factorization

$$(t_-z_-{\rm i}\,\sin\varphi)^2=(t_+z_+-\lambda_+)^2-t_-^2z_-^2=(\lambda_{{\rm s},+}-\lambda_+)(\lambda_{{\rm d},+}-\lambda_+), \tag{D.6}$$

as $\lambda_{{\rm s},+}=t_+z_++t_-z_-$ and $\lambda_{{\rm d},+}=t_+z_+-t_-z_-$, we deduce the closed form expression

$$\begin{aligned}\prod_{\mu=1}^{M}(t_-z_-{\rm i}\,\sin\varphi_\mu)^2&=\prod_{\mu=1}^{M}(\lambda_{{\rm s},+}-\lambda_{\mu,+})(\lambda_{{\rm d},+}-\lambda_{\mu,+})=P_{\boldsymbol{\lambda}_+}(\lambda_{{\rm s},+})P_{\boldsymbol{\lambda}_+}(\lambda_{{\rm d},+})\\&=(1-t^{*2})^2\left(\frac{t_-z_-}{2}\right)^{2M}\left(1-M\frac{\lambda_{{\rm s},-}}{z_-}\right)\left(1+M\frac{\lambda_{{\rm d},-}}{z_-}\right).\end{aligned} \tag{D.7}$$

ORCID iDs

Alfred Hucht https://orcid.org/0000-0002-9276-0159

References

[1] Ising E 1925 Beitrag zur Theorie des Ferromagnetismus *Z. Phys.* **31** 253
[2] Onsager L 1944 Crystal statistics. I. A two-dimensional model with an order–disorder transition *Phys. Rev.* **65** 117
[3] Kaufman B 1949 Crystal statistics. II. Partition function evaluated by spinor analysis *Phys. Rev.* **76** 1232–43
[4] McCoy B M and Wu T T 1973 *The Two-Dimensional Ising Model* (Cambridge, MA: Harvard University Press)
[5] Baxter R J 1982 *Exactly Solved Models in Statistical Mechanics* (London: Academic)
[6] Abraham D B 1986 Surface structures and phase transitions—exact results *Phase Transition and Critical Phenomena* vol 10 ed C Domb and J L Lebowitz (London: Academic) pp 1–74
[7] Baxter R J 2017 The bulk, surface and corner free energies of the square lattice Ising model *J. Phys. A: Math. Theor.* **50** 014001

[8] Baxter R J 2020 The bulk, surface and corner free energies of the anisotropic triangular Ising model *Proc. R. Soc.* A **476** 20190713
[9] Hucht A 2017 The square lattice Ising model on the rectangle I: finite systems *J. Phys. A: Math. Theor.* **50** 065201
[10] Hucht A 2018 Erratum: the square lattice Ising model on the rectangle I: finite systems *J. Phys. A: Math. Theor.* **51** 319601
[11] Hucht A 2017 The square lattice Ising model on the rectangle II: finite-size scaling limit *J. Phys. A: Math. Theor.* **50** 265205
[12] Vernier E and Jacobsen J L 2012 Corner free energies and boundary effects for Ising, Potts and fully packed loop models on the square and triangular lattices *J. Phys. A: Math. Theor.* **45** 045003
[13] Kasteleyn P W 1961 The statistics of dimers on a lattice *Physica* **27** 1209–25
[14] Kasteleyn P W 1963 Dimer statistics and phase transitions *J. Math. Phys.* **4** 287
[15] Fisher M E 1966 On the dimer solution of planar Ising models *J. Math. Phys.* **7** 1776–81
[16] McCoy B M and Wu T T 2014 *The Two-Dimensional Ising Model* (*Dover Books on Physics*) (New York: Dover)
[17] Molinari L G 2008 Determinants of block tridiagonal matrices *Linear Algebra and its Applications* **429** 2221
[18] Fisher M E and de Gennes P-G 1978 Phénomènes aux parois dans un mélange binaire critique *C. R. Acad. Sci. Paris* B **287** 207
[19] Fisher M E and Au-Yang H 1980 Critical wall perturbations and a local free energy functional *Physica* A **101** 255–64
[20] Casimir H B G and Polder D 1948 The influence of retardation on the London–van der Waals forces *Phys. Rev.* **73** 360–72
[21] Casimir H B G 1948 On the attraction between two perfectly conducting plates *Proc. K. Ned. Akad. Wet.* **51** 793
[22] Hucht A, Grüneberg D and Schmidt F M 2011 Aspect-ratio dependence of thermodynamic Casimir forces *Phys. Rev.* E **83** 051101
[23] Kadanoff L P 1966 Scaling laws for Ising models near T_c *Physics* **2** 263
[24] Diehl H W 1997 The theory of boundary critical phenomena *Int. J. Mod. Phys.* B **11** 3503–23
[25] Evans R and Stecki J 1994 Solvation force in two-dimensional Ising strips *Phys. Rev.* B **49** 8842–51
[26] Au-Yang H and Fisher M E 1980 Wall effects in critical systems: scaling in Ising model strips *Phys. Rev.* B **21** 3956
[27] Brankov J G, Dantchev D M and Tonchev N S 2000 *Theory of Critical Phenomena in Finite-Size Systems—Scaling and Quantum Effects* (Singapore: World Scientific)
[28] Gambassi A 2009 The Casimir effect: from quantum to critical fluctuations *J. Phys.: Conf. Ser.* **161** 012037
[29] Rudnick J, Zandi R, Shackell A and Abraham D B 2010 Boundary conditions and the critical Casimir force on an Ising model film: exact results in one and two dimensions *Phys. Rev.* E **82** 041118
[30] Abraham D B and Maciołek A 2010 Casimir interactions in Ising strips with boundary fields: exact results *Phys. Rev. Lett.* **105** 055701
[31] Abraham D B and Maciołek A 2013 Surface states and the Casimir interaction in the Ising model *Europhys. Lett.* **101** 20006
[32] Hasenbusch M 2009 The thermodynamic Casimir effect in the neighbourhood of the lambda-transition: a Monte Carlo study of an improved three-dimensional lattice model *J. Stat. Mech.* P07031
[33] Hasenbusch M 2010 Specific heat, internal energy, and the thermodynamic Casimir force in the neighbourhood of the lambda transition *Phys. Rev.* B **81** 165412
[34] Hasenbusch M 2009 Yet another method to compute the thermodynamic Casimir force in lattice models *Phys. Rev.* E **80** 061120
[35] Hasenbusch M 2010 Thermodynamic Casimir effect for films in the three-dimensional Ising universality class: symmetry-breaking boundary conditions *Phys. Rev.* B **82** 104425
[36] Hasenbusch M 2011 Thermodynamic Casimir force: a Monte Carlo study of the crossover between the ordinary and the normal surface universality class *Phys. Rev.* B **83** 134425
[37] Hasenbusch M 2012 Thermodynamic Casimir effect: universality and corrections to scaling *Phys. Rev.* B **85** 174421
[38] Hucht A 2007 Thermodynamic Casimir effect in ^{4}He films near T_λ: Monte Carlo results *Phys. Rev. Lett.* **99** 185301

[39] Maciołek A, Gambassi A and Dietrich S 2007 Critical Casimir effect in superfluid wetting films *Phys. Rev.* E **76** 031124
[40] Vasilyev O, Gambassi A, Maciołek A and Dietrich S 2007 Monte Carlo simulation results for critical Casimir forces *Europhys. Lett.* **80** 60009
[41] Vasilyev O, Gambassi A, Maciołek A and Dietrich S 2009 Universal scaling functions of critical Casimir forces obtained by Monte Carlo simulations *Phys. Rev.* E **79** 041142
[42] Hobrecht H and Hucht A 2014 Direct simulation of critical Casimir forces *Europhys. Lett.* **106** 56005
[43] Garcia R and Chan M H W 1999 Critical fluctuation-induced thinning of ^{4}He films near the superfluid transition *Phys. Rev. Lett.* **83** 1187
[44] Garcia R and Chan M H W 2000 Critical Casimir effect in dilute ^{3}He–^{4}He mixture films *Physica* B **280** 55
[45] Garcia R and Chan M H W 2000 Preliminary measurement of the critical Casimir effect near the tricritical point in ^{3}He–^{4}He mixture films *J. Low Temp. Phys.* **121** 495–500
[46] Garcia R and Chan M H W 2002 Critical Casimir effect near the ^{3}He–^{4}He tricritical point *Phys. Rev. Lett.* **88** 086101
[47] Fukuto M, Yano Y F and Pershan P S 2005 Critical Casimir effect in three-dimensional Ising systems: measurements on binary wetting films *Phys. Rev. Lett.* **94** 135702
[48] Ganshin A, Scheidemantel S, Garcia R and Chan M H W 2006 Critical Casimir force in ^{4}He films: confirmation of finite-size scaling *Phys. Rev. Lett.* **97** 075301
[49] Hertlein C, Helden L, Gambassi A, Dietrich S and Bechinger C 2008 Direct measurement of critical Casimir forces *Nature* **451** 172
[50] Gambassi A, Maciołek A, Hertlein C, Nellen U, Helden L, Bechinger C and Dietrich S 2009 Critical Casimir effect in classical binary liquid mixtures *Phys. Rev.* E **80** 061143
[51] Polyakov A M 1970 Conformal symmetry of critical fluctuations *JETP Lett.* **12** 381
[52] Cardy J L 1984 Conformal invariance and universality in finite-size scaling *J. Phys. A: Math. Gen.* **17** L385
[53] Burkhardt T W and Eisenriegler E 1995 Casimir interaction of spheres in a fluid at the critical point *Phys. Rev. Lett.* **74** 3189–92
[54] Cardy J 2006 Boundary conformal field theory *Encyclopedia of Mathematical Physics* ed J-P Françoise, G L Naber and T S Tsun (London: Academic) pp 333–40
[55] Bimonte G, Emig T and Kardar M 2013 Conformal field theory of critical Casimir interactions in 2D *Europhys. Lett.* **104** 21001
[56] Ferdinand A E and Fisher M E 1969 Bounded and inhomogeneous Ising models. I. Specific-heat anomaly of a finite lattice *Phys. Rev.* **185** 832
[57] Lu W T and Wu F Y 2001 Ising model on nonorientable surfaces: exact solution for the Möbius strip and the Klein bottle *Phys. Rev.* E **63** 026107
[58] Kleban P and Vassileva I 1991 Free energy of rectangular domains at criticality *J. Phys. A: Math. Gen.* **24** 3407
[59] Wu X, Izmailian N and Guo W 2012 Finite-size behavior of the critical Ising model on a rectangle with free boundaries *Phys. Rev.* E **86** 041149
[60] Schlesener F, Hanke A and Dietrich S 2003 Critical Casimir forces in colloidal suspensions *J. Stat. Phys.* **110** 981–1013
[61] Kondrat S, Harnau L and Dietrich S 2009 Critical Casimir interaction of ellipsoidal colloids with a planar wall *J. Chem. Phys.* **131** 204902
[62] Tröndle M, Kondrat S, Gambassi A, Harnau L and Dietrich S 2009 Normal and lateral critical Casimir forces between colloids and patterned substrates *Europhys. Lett.* **88** 40004
[63] Gambassi A and Dietrich S 2010 Colloidal aggregation and critical Casimir forces *Phys. Rev. Lett.* **105** 059601
[64] Tröndle M, Zvyagolskaya O, Gambassi A, Vogt D, Harnau L, Bechinger C and Dietrich S 2011 Trapping colloids near chemical stripes via critical Casimir forces *Mol. Phys.* **109** 1169–85
[65] Hasenbusch M 2013 Thermodynamic Casimir forces between a sphere and a plate: Monte Carlo simulation of a spin model *Phys. Rev.* E **87** 022130
[66] Labbé-Laurent M, Tröndle M, Harnau L and Dietrich S 2014 Alignment of cylindrical colloids near chemically patterned substrates induced by critical Casimir torques *Soft Matter* **10** 2270–91
[67] Hobrecht H and Hucht A 2015 Many-body critical Casimir interactions in colloidal suspensions *Phys. Rev.* E **92** 042315

[68] Edison J R, Tasios N, Belli S, Evans R, van Roij R and Dijkstra M 2015 Critical Casimir forces and colloidal phase transitions in a near-critical solvent: a simple model reveals a rich phase diagram *Phys. Rev. Lett.* **114** 038301
[69] Brunner M, Dobnikar J, von Grünberg H-H and Bechinger C 2004 Direct measurement of three-body interactions amongst charged colloids *Phys. Rev. Lett.* **92** 078301
[70] Soyka F, Zvyagolskaya O, Hertlein C, Helden L and Bechinger C 2008 Critical Casimir forces in colloidal suspensions on chemically patterned surfaces *Phys. Rev. Lett.* **101** 208301
[71] Bonn D, Otwinowski J, Sacanna S, Guo H, Wegdam G and Schall P 2009 Direct observation of colloidal aggregation by critical Casimir forces *Phys. Rev. Lett.* **103** 156101
[72] Zvyagolskaya O, Archer A J and Bechinger C 2011 Criticality and phase separation in a two-dimensional binary colloidal fluid induced by the solvent critical behavior *Europhys. Lett.* **96** 28005
[73] Gnan N, Zaccarelli E and Sciortino F 2012 Tuning effective interactions close to the critical point in colloidal suspensions *J. Chem. Phys.* **137** 084903
[74] Gnan N, Zaccarelli E, Tartaglia P and Sciortino F 2012 How properties of interacting depletant particles control aggregation of hard-sphere colloids *Soft Matter* **8** 1991–6
[75] Dang M T, Verde A V, Nguyen V D, Bolhuis P G and Schall P 2013 Temperature-sensitive colloidal phase behavior induced by critical Casimir forces *J. Chem. Phys.* **139** 094903
[76] Nguyen V D, Faber S, Hu Z, Wegdam G H and Schall P 2013 Controlling colloidal phase transitions with critical Casimir forces *Nat. Commun.* **4** 1584
[77] Tasios N and Dijkstra M 2017 From 2D to 3D: critical Casimir interactions and phase behavior of colloidal hard spheres in a near-critical solvent *J. Chem. Phys.* **146** 134903
[78] Hobrecht H and Hucht A 2017 Critical Casimir force scaling functions of the two-dimensional Ising model at finite aspect ratios *J. Stat. Mech.* 024002
[79] Hobrecht H and Hucht A 2019 Anisotropic scaling of the two-dimensional Ising model I: the torus *SciPost Phys.* **7** 26
[80] Hobrecht H and Hucht A 2020 Anisotropic scaling of the two-dimensional Ising model II: surfaces and boundary fields *SciPost Phys.* **8** 32
[81] Lawden D F 1989 *Elliptic Functions and Applications* (*Applied Mathematical Sciences*) (New York: Springer)
[82] Olver F W J, Lozier D, Boisvert R and Clark C 2010 *NIST Handbook of Mathematical Functions* (Cambridge: Cambridge University Press)
[83] Olver F W J *et al* (ed) *NIST Digital Library of Mathematical Functions* http://dlmf.nist.gov/ release 1.1.1 of 15-03-2021
[84] Iorgov N and Lisovyy O 2011 Ising correlations and elliptic determinants *J. Stat. Phys.* **143** 33
[85] Bultheel A and van Barel M 2011 *Linear Algebra, Rational Approximation and Orthogonal Polynomials* (Amsterdam: North-Holland)
[86] Wolfram Research, Inc. 2020 *Mathematica Version 12.2* (Champaign, Illinois: Wolfram Research)
[87] Parlett B N 1980 *The Symmetric Eigenvalue Problem SIAM Classics in Applied Mathematics* (Philadelphia, PA: SIAM)
[88] Heinig G and Rost K 2000 *Bezoutians* (Germany: Technische Universität Chemnitz, Fakultät für Mathematik)
[89] Luther U and Rost K 2004 Matrix exponentials and inversion of confluent Vandermonde matrices *Electron. Trans. Numer. Anal.* **18** 91–100
[90] Fisher M E and Hartwig R E 1968 Toeplitz determinants: some applications, theorems and conjectures *Adv. Chem. Phys.* **15** 333–53
[91] Hartwig R E and Fisher M E 1969 Asymptotic behavior of Toeplitz matrices and determinants *Arch. Ration. Mech. Anal.* **32** 190–225
[92] Basor E L and Ehrhardt T 2002 Some identities for determinants of structured matrices *Linear Algebra Appl.* **343–344** 5–19 Special issue on structured and infinite systems of linear equations
[93] Deift P, Its A and Krasovsky I 2013 Toeplitz matrices and Toeplitz determinants under the impetus of the Ising model: some history and some recent results *Commun. Pure Appl. Math.* **66** 1360–438
[94] Szegő G 1915 Ein Grenzwertsatz über die Toeplitzschen Determinanten einer reellen positiven Funktion *Math. Ann.* **76** 490–503
[95] Szegő G 1920 Beiträge zur Theorie der Toeplitzschen Formen, I *Math. Zeit.* **6** 167–202